NAVAL POSTGRADUATE SCHOOL

Monterey, California

THESIS

A CALORIMETRIC STUDY OF THE MICROSTRUCTURES OF A THERMOMECHANICALLY PROCESSED Al-10% Mg-0.1% Zr ALLOY

by

James N. Andrews, Jr.

September 1986

Thesis Advisor: T. R. McNelley

Approved for public release; distribution is unlimited.

UNCLASSIFIED

SECURITY CLASSIFICATION OF THIS PAGE

REPORT DOCUMENTATION PAGE

1a REPORT SECURITY CLASSIFICATION Unclassified	1b. RESTRICTIVE MARKINGS
2a. SECURITY CLASSIFICATION AUTHORITY	3 DISTRIBUTION / AVAILABILITY OF REPORT Approved for public release; Distribution is unlimited
2b. DECLASSIFICATION / DOWNGRADING SCHEDULE	
4 PERFORMING ORGANIZATION REPORT NUMBER(S)	5. MONITORING ORGANIZATION REPORT NUMBER(S)
6a. NAME OF PERFORMING ORGANIZATION Naval Postgraduate School 6b OFFICE SYMBOL (If applicable) 69	7a. NAME OF MONITORING ORGANIZATION Naval Postgraduate School
6c. ADDRESS (City, State, and ZIP Code) Monterey, CA 93943-5000	7b. ADDRESS (City, State, and ZIP Code) Monterey, CA 93943-5000
8a. NAME OF FUNDING / SPONSORING ORGANIZATION 8b. OFFICE SYMBOL (If applicable)	9. PROCUREMENT INSTRUMENT IDENTIFICATION NUMBER
8c. ADDRESS (City, State, and ZIP Code)	10 SOURCE OF FUNDING NUMBERS PROGRAM ELEMENT NO / PROJECT NO / TASK NO / WORK UNIT ACCESSION NO

11 TITLE (Include Security Classification)
A CALORIMETRIC STUDY OF THE MICROSTRUCTURES OF A THERMOMECHANICALLY PROCESSED Al-10.0% Mg-0.1% Zr ALLOY

12 PERSONAL AUTHOR(S)
JAMES N. ANDREWS

13a TYPE OF REPORT	13b TIME COVERED	14 DATE OF REPORT (Year, Month, Day)	15 PAGE COUNT
Masters Thesis	FROM _____ TO _____	September 1986	51

16 SUPPLEMENTARY NOTATION

17 COSATI CODES			18 SUBJECT TERMS (Continue on reverse if necessary and identify by block number)
FIELD	GROUP	SUB-GROUP	Superplasticity, Aluminum Alloys, Aluminum-Magnesium, Thermomechanical Processing, Differential Scanning Calorimetry

19 ABSTRACT (Continue on reverse if necessary and identify by block number)

Differential scanning calorimetry (DSC) was used to investigate microstructure evolution in a high-magnesium aluminum-magnesium alloy, Al-10.0% Mg-0.1% Zr, which had been thermomechanically processed. The two variations of the thermomechanical processing (TMP) investigated resulted in an extremely fine grain size, one of the preconditions for superplastic deformation. The DSC results were consistent with previous research indicating continuous recrystallization occurs during annealing and deformation at relatively low temperatures. Additional insight into the development of the microstructure produced by the two TMP variations was obtained, especiallly with regard to the intermetallic β-phase. The DSC study also showed that a morphological difference exists in the microstructures produced by the two TMP variations used, and transmission electron microscopy (TEM) results confirmed these differences.

20 DISTRIBUTION / AVAILABILITY OF ABSTRACT	21 ABSTRACT SECURITY CLASSIFICATION
☒ UNCLASSIFIED/UNLIMITED ☐ SAME AS RPT. ☐ DTIC USERS	Unclassified
22a NAME OF RESPONSIBLE INDIVIDUAL Professor T. R. McNelley	22b TELEPHONE (Include Area Code) (408) 646-2589 22c OFFICE SYMBOL 69Mc

DD FORM 1473, 84 MAR 83 APR edition may be used until exhausted
All other editions are obsolete

SECURITY CLASSIFICATION OF THIS PAGE
UNCLASSIFIED

Approved for public release; distribution is unlimited.

A Calorimetric Study of the Microstructures of a
Thermomechanically Processed Al-10.0% Mg-0.1% Zr Alloy

by

James N. Andrews, Jr.
Lieutenant Commander, United States Navy
B.S., United States Naval Academy, 1974

Submitted in partial fulfillment of the
requirements for the degree of

MASTER OF SCIENCE IN MECHANICAL ENGINEERING

from the

NAVAL POSTGRADUATE SCHOOL
September 1986

Author: _____
James N. Andrews, Jr.

Approved by: _____
T. R. McNelley, Thesis Advisor

_____
A. J. Healey, Chairman,
Department of Mechanical Engineering

_____
John N. Dyer,
Dean of Science and Engineering

ABSTRACT

Differential scanning calorimetry (DSC) was used to investigate microstructure evolution in a high-magnesium aluminum-magnesium alloy, Al-10.0% Mg-0.1% Zr, which had been thermomechanically processed. The two variations of the thermomechanical processing (TMP) investigated resulted in an extremely fine grain size, one the preconditions for superplastic deformation. The DSC results were consistent with previous research indicating continuous recrystallization occurs during annealing and deformation at relatively low temperatures. Additional insight into the development of the microstructure produced by the two TMP variations was obtained, especially with regard to the intermetallic β-phase. The DSC study also showed that a morphological difference exists in the microstructures produced by the two TMP variations used, and transmission electron microscopy (TEM) results confirmed these differences.

TABLE OF CONTENTS

LIST OF FIGURES

I. INTRODUCTION

Mankind, in the pursuit of "a better mousetrap", has developed a wide array of engineering materials which possess various traits. Improvements in strength, reduced weight, resistance to fatigue and corrosion, machinability, ductility and toughness have been general goals in the continuing search for new materials. Aluminum moved into the forefront in the early part of this century with numerous aluminum alloys having been developed for industrial use.

Superplasticity, the ability of some materials to sustain elongations of several hundred percent under certain temperature and strain rate conditions, provides a means of further enhancing the performance of selected materials. This behavior in metals was merely a laboratory curiosity when first observed in a cold-rolled zinc-copper-aluminum ternary eutectic alloy by Rosenhain as reported by Johnson [Ref. 1:p. 115] in 1920. Underwood [Ref. 2] kindled the most recent interest by reviewing the work performed in the Soviet Union in the 1940's. Initially thought to be confined to eutectic alloys, superplastic deformation has been obtained in other alloy types. Superplasticity has been applied commercially to aluminum alloys, titanium alloys, and nickel-based superalloys. Research in superplasticity has increased with the growth in commercial interest. The ability to form complex shapes with excellent dimensional accuracy and to produce smooth surfaces in a small number of operations using relatively inexpensive tooling equates to reduced costs and increased profits for industry. Of prime interest is the application of superplasticity to the formation of components for the aerospace industry, where the elimination of fasteners gives rise to reductions in weight and stress concentraters in the structure.

The universally acknowledged prerequisite for superplastic deformation is an equiaxed, fine-sized grain structure which is stable at the deformation temperature. Control of the microstructure is essential to the understanding and application of superplasticity. Research at the Naval Postgraduate School has produced a high-Mg, Al-Mg-Zr alloy which can be superplastically deformed when properly thermomechanically processed. The focus of this thesis is to gain a further insight into the microstructure and microstructure evolution in this Al-Mg-Zr alloy through the use of differential scanning calorimetry complemented by transmission electron microscopy.

II. BACKGROUND

A. PHYSICAL METALLURGY

1. Aluminum Alloy Systems

Aluminum alloys are used extensively in industry, ranking second to iron and steel in terms of volume and weight [Ref. 3:p. 6.1]. Their popularity stems from the good strength to weight ratio, ease of machining, weldability and resistance to corrosion and fatigue. Classed into two groups, wrought aluminum alloys are considered heat-treatable or non-heat-treatable based upon the means of strengthening employed. A heat-treatable Al alloy is strengthened by precipitation hardening, while a non-heat-treatable Al alloy must be strengthened by solution hardening or strain hardening.

2. Alloy Strengthening

In pure metals, dislocations are quite mobile through the crystalline lattice. Consequently, plastic deformation readily occurs, and those materials have little strength. Strength is imparted when the motion of dislocations is restricted in some manner.

a. Solid Solution Strengthening

When solute atoms are introduced into a solid, the result is an increase in strength. This strengthening occurs as the solute atoms interact with dislocations and restrict their motion. The degree to which solute atoms restrict dislocation mobility is dependent upon the relative contributions of the following mechanisms [Ref. 4:pp. 387-393]:

1) elastic interaction
2) modulus difference interaction
3) electrical interaction
4) chemical (Suzuki) interaction
5) local order interaction.

All Al alloys are strengthened to some degree by the solid solution mechanism.

b. Precipitation Strengthening

Precipitation hardening, or age hardening, results from the presence of second phase particles which interact with dislocations and restrict their mobility. The second phase must exhibit decreasing solubility with decreasing temperature. Precipitation occurs when the alloy is heated to form a single phase, rapidly cooled, and then reheated to ~ 0.4 T_m, where T_m is the absolute melting temperature of the alloy. The strengthening second phase particles, or precipitates, are usually coherent with the matrix, resulting in an elastic strain field which also interacts with dislocations to increase strength. This is the primary strengthening mechanism for many high-strength Al alloys.

c. Dispersion Strengthening

Dispersion strengthening, like precipitation hardening, relies on particles to restrict dislocation mobility, thereby imparting strength to the alloy. Unlike precipitation hardening, however, the dispersion hardening particle, or dispersoid, is much harder than the matrix and is insoluble even at high temperatures. The dispersoids are a fine size and are incoherent with the matrix. Dispersoids also may be introduced to inhibit recrystallization.

3. Effect of Alloying Elements

a. Magnesium

The addition of magnesium to Al produces alloys which have moderate strength with good ductility, with additional strength attainable through cold work and excellent corrosion resistance and weldability. Magnesium's density and modulus of elasticity are lower than aluminum's, resulting in decreases in those properties for the solid solution. Strengthening is by solid solution hardening, and some precipitation hardening may occur for > 7% Mg [Ref. 5:p. 174]. Mondolfo [Ref. 6:p. 312] described the precipitation of a second phase as:

$$\text{Supersaturated solution} \rightarrow \text{Al} + \beta\ (Mg_5Al_8)$$

The precipitation of β during processing of Al-Mg-X alloys at NPS has been an important factor in achieving superplasticity.

b. Zirconium

Added to the Al-Mg binary alloy, zirconium acts as a grain refiner. The precipitation of a second phase, $ZrAl_3$, occurs at extremely high temperatures. When present as a fine dispersoid, $ZrAl_3$, increases the recrystallization temperature [Ref. 6:p.

414]. The presence of the dispersoid can control recrystallization during processing [Ref. 7:p. 2320] which will prove beneficial in achieving the required grain structure for superplastic deformation.

B. SUPERPLASTICITY

1. Phenomenology

As yet no single explanation for superplasticity has been universally accepted; however, most relationships, which are phenomenological in nature, are centered about the power of Backofen, Turner, and Avery [Ref. 8:p. 980]·

$$\sigma = k\dot{\varepsilon}^m$$

where σ is the flow stress, k is a temperature dependent material constant, and ε is the strain rate, and m is a strain-rate sensitivity coefficient.

The current theories all consider grain boundary sliding accommodated by some additional mechanism as the explanation for superplastic flow [Ref. 9:pp. 30-32]. Most widely accepted are the relations [Ref. 10:p. 242]:

$$\dot{\varepsilon} = D_{gb}\sigma^2/d^3$$

or

$$\dot{\varepsilon} = D_L\sigma^2/d^2$$

for the cases of superplastic flow rate-controlled by grain boundary diffusion or lattice diffusion, respectively. For either of the above cases, superplastic flow is strongly dependent upon grain size.

2. Microstructure

There is general agreement on the microstructural prerequisites for superplastic deformation [Refs. 11,12,13:pp. 151-152,68-69,367-370]:

1) equiaxed, fine grain size (< 10 μm) with high angle boundaries
2) grain structure stable at deformation temperature
3) deformable, dispersed second phase (if present)
4) high resistance to cavitation.

Attainment of these conditions entails some form of grain refinement before deformation occurs, and microstructural stability at the deformation temperature is limited by grain coarsening or recrystallization which may occur at proximate temperatures. To stabilize the grain size prior to and during deformation, some form of grain boundary pinning is required. An understanding of the evolution of the microstructure at those temperatures is essential to adequately control it.

a. Recovery

Plastic deformation of an alloy produces an increase in the dislocation density. Recovery occurs to reduce the density and to arrange defects introduced during deformation. Thus there exists a driving force, the high internal energy stored during deformation, to return the alloy to a lower energy state [Ref. 14:pp. 2-3]. Dislocations are reduced in number through annihilation by mutual interaction or by rearrangement into a lower energy configuration. The rearrangement results in a cellular structure with relatively dislocation-free interiors. This process is termed polygonization [Ref. 4:p. 377]. The resultant structure has boundaries with orientation differences $< 5°$ [Ref. 15:p. 192].

b. Recrystallization

Recrystallization occurs when new, less distorted grains form; generally, the misorientations of the adjacent grains exceeds 10° [Ref. 15:p. 192]. Two modes of recrystallization have been observed in alloys.

(1) *Discontinuous Recrystallization.* Discontinuous recrystallization is the classical mode where new, strain-free grains nucleate and then grow. This occurs as a high-angle grain boundary migrates through a deformed region. The migration results in abrupt changes in the crystallographic orientation of adjacent grains and in the reduced dislocation densities. This mode can be used for microstructural control, but it often results in relatively large grain sizes unless significant grain boundary pinning occurs.

(2) *Continuous Recrystallization.* Continuous recrystallization is the gradual evolution of a grain structure from a recovered state ; therefore, nucleation and growth is not involved. By continuous recrystallization, high-angle grain boundaries evolve from the gradual increase in misorientation between adjacent subgrains. This can only occur when the relatively more rapid process of discontinuous recrystallization is suppressed [Ref. 12:pp. 75]. Continuous recrystallization has been observed in other

superplastic Al alloys by Ahlborn *et al.* [Ref. 16:p. 944], Nes [Ref. 17:p. 2055], and Watts *et al.* [Refs. 18,19:pp. 196,205].

3. Thermomechanical Processing

Most technologically important superplastic alloys require some type of processing before they exhibit superplastic behavior. This is true even if their elemental constituents make them candidates for superplastic deformation. For the Al-Mg-Zr alloy developed at NPS, two thermomechanical processing (TMP) variations have been employed [Ref. 20:pp. 24-27]. Figure 2.1 shows the region of the Al-Mg phase diagram in which the processing takes place. The TMP is schematically represented in Figure 2.2. The variations differ only in the warm rolling portion of the TMP. Both variations result in the same reduction and total strain for the material. The light reduction schedule reduces the alloy 1 mm per rolling pass. This takes approximately 28 rolling passes, and the material is subjected to the warm rolling temperature for about 120 minutes. The heavy reduction schedule uses a constant reduction of 2 mm per rolling pass. The required number of rolling passes is less, 10-12, and the material is subjected to the warm rolling temperature for approximately 70-80 minutes.

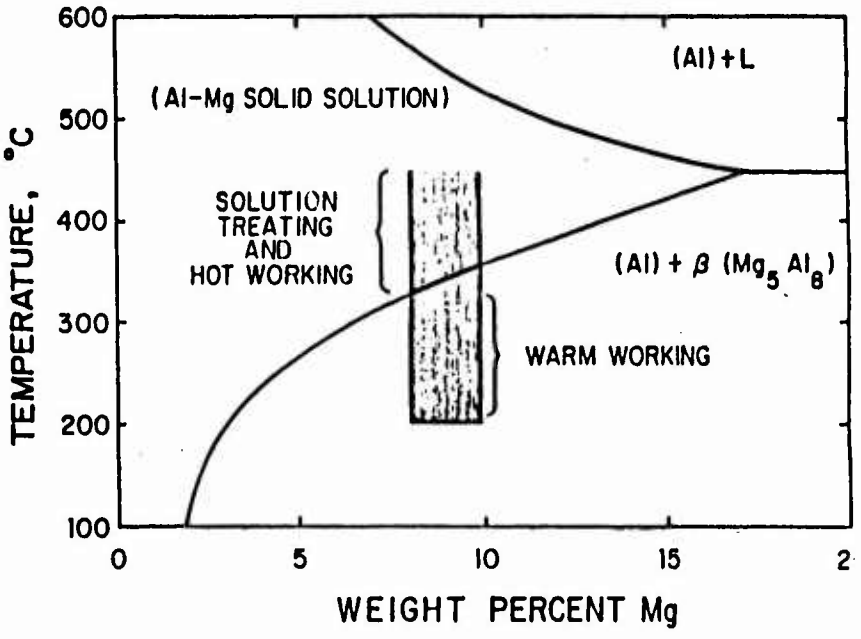

Figure 2.1 Aluminum-Magnesium phase diagram with TMP region indicated.

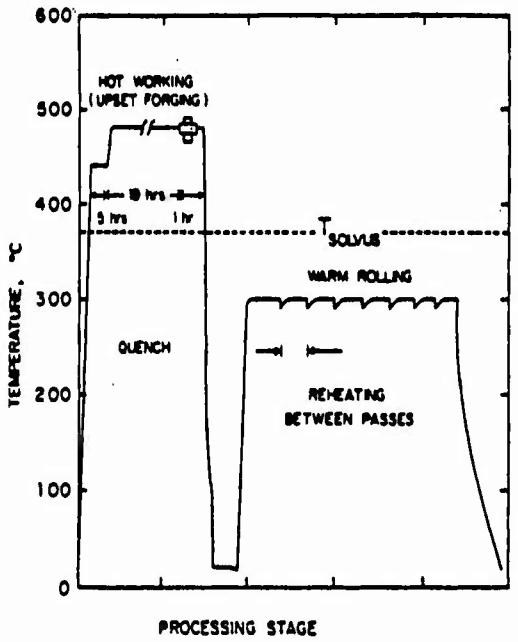

Figure 2.2 Schematic of the thermomechanical processing technique.

C. DIFFERENTIAL SCANNING CALORIMETRY

Several thermal analysis techniques are available to observe reactions which occur due to a change in temperature. Differential scanning calorimetry (DSC) is a technique that employs energy differences to indicate the changes. In DSC, the material of interest and a reference material are placed into separate sample pans with covers. The pans are placed in individual holders in a thermal block which is under a dynamic atmosphere of inert gas. The materials are then heated, or cooled, at a programmed rate by individual heaters. This arrangement is illustrated schematically in Figure 2.3. A dual- loop control system ensures the samples are kept at the same temperatures while the programmed heating (or cooling) rate is maintained. Any difference in power required to maintain the same temperature and heating rate for the sample and reference is sensed by the instrument and is registered as a proportional signal on an appropriate recording device. A power deficit indicates an endothermic reaction; a power excess, an exothermic reaction. Calculations can be made from these outputs to determine specific heat or energies associated with the reactions. [Ref. 21]

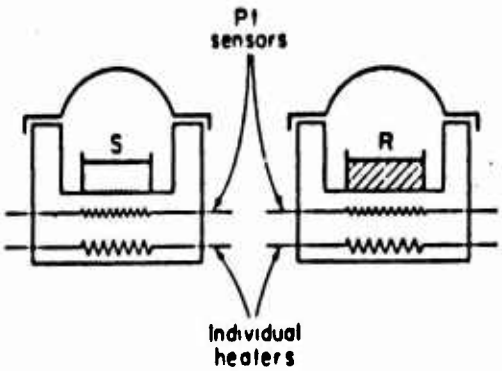

Figure 2.3 Differential scanning calorimeter schematic.
S is sample material. R is reference material.

III. EXPERIMENTAL PROCEDURES

A. MATERIAL

The nominal composition of the alloy studied was 10.0 weight percent magnesium and 0.1 percent zirconium. ALCOA Technical center, Alcoa Center, Pa. produced the direct-chill cast ingot using 99.99% pure aluminum base metal alloyed with commercially pure magnesium, aluminum-zirconium master alloy, titanium-boron addition for grain size control in the as-cast condition, and beryllium as 5% Be aluminum-beryllium master alloy for oxidation control. [Ref. 22] The complete chemical composition of the alloy is shown below:

Ingot No.	Si	Fe	Mg	Zr	Zn	Ti	Al
572876	0.02	0.02	9.90	0.09	0.01	0.01	Bal

The material studied had been thermomechanically processed previously by Grider [Ref. 20:pp. 26-27] and Klankowski [Ref. 23:pp. 23-25]. The thermomechanical processing, represented in Figure 2.2, produced two variations of the material. Samples were tested from both of the TMP variations.

B. SAMPLE PREPARATION

Two types of samples were prepared from the as-rolled material for study in the differential scanning calorimeter. The first type was a bulk sample cut utilizing a high-concentration diamond wafering blade in a low speed saw. The bulk sample dimensions were approximately 3.2mm x 3.2 mm x 0.95 mm. Smoothing was done by wet sanding on 600 grit silicon carbide abrasive paper to maximize sample-to-pan contact in the calorimeter. Bulk specimens were made only from the heavy reduction material. Thin disc specimens were prepared from both TMP variation materials by wafering the as-rolled material parallel to the long transverse direction to a thickness of about 0.35 mm. Further reduction in thickness to 0.30 mm was accomplished by mechanical grinding on fine grit silicon carbide paper. The discs were then punched to a diameter of 3.0 mm using a through-type punch.

Foils for transmission electron microscopy (TEM) were prepared by twin-jet polishing in a Struers Tenupol 2 Electro-Thinning unit. A setting of 15 vdc was used, and a solution of 25% HNO_3 in methanol cooled to $-20°C$ was the electrolyte.

C. CALORIMETRY AND MICROSCOPY

Calorimetric measurements were made using a Perkin-Elmer DSC-2C Differential Scanning Calorimeter with a Perkin-Elmer Scanning AutoZero accessory attached. The DSC results were recorded on a two-pen Perkin-Elmer Model 56 strip-chart recorder. Specimens were placed in aluminum sample pans with aluminum covers. A high purity aluminum disc of approximately the same mass was used as a reference for the bulk specimens. The weight of the thin discs were small enough that an empty sample pan and cover served as the reference. The sample holder was kept under a dynamic atmosphere of dry argon flowing at 20 ml/min. A temperature range of 323-723K (50°-450°C) was scanned at programmed rates of 40K/min. and 80K/min.

Examination and micrographic work was accomplished using a JEOL JEM-100CX II electron microscope. An accelerating voltage of 120 kV was employed.

D. DATA REDUCTION

After a DSC run was completed the data were corrected for any temperature dependence of the solid solution by subtracting a baseline value obtained from a second heating cycle applied to the sample. The basis for this will be discussed in the next chapter. This was done so that the data for the first cycle reflected the reactions which had taken place during that cycle. The data were subsequently converted to ΔC_p *vs.* temperature plots by the below equation:

$$\Delta C_p = (dH/dt)m^{-1}(dT/dt)^{-1}$$

where dH/dt is the pen deflection from the baseline, m is the sample mass and dT/dt is the programmed scanning rate.

IV. RESULTS AND DISCUSSION

A. ESTABLISHMENT OF DSC BASELINE

Materials processed by the two thermomechanical processing (TMP) variations were tested in the differential scanning calorimeter (DSC) as shown schematically in Figure 4.1. During the first cycle the sample was heated to the upper temperature limit, 723K (450°C), at a rate (40K/min) sufficient to observe the various solid state reactions which occur in that temperature range. These reactions are seen in Figure 4.2. Returning to room temperature after heating to 723K, the microscopy, as shown in Figure 4.3, indicates the material to be fully annealed and solution treated. Cooling the alloy at 40K/min apparently has precluded the reprecipitation of any intermetallic β phase. Previous research by McNelley and Garg [Ref. 24:p. 918] also indicated that Mg was retained in solid solution when the alloy was quenched following solution treatment. Therefore, no reactions should be observed during the heating portion of the second cycle. The recorder trace of the second heating cycle, Figure 4.4, was essentially free of any indications of solid state reactions. Any activity registered on the recorder trace of the first cycle, then, can be measured from the baseline established by the second cycle trace, and the changes which occurred should reflect only the internal changes of the alloy. These reactions are shown in Figure 4.5, where the second cycle trace has been manually superimposed on the first cycle trace.

Examination of the DSC trace revealed endothermic peaks at opposite ends of the temperature range and a shallow exothermic deflection between them. The initial endothermic peak occurred over the temperature range 362-394K (89°-121°C). The exothermic peak occurred over the temperature range 396-545K (123°-272°C). The second endothermic peak was a doublet peak which extended over the temperature range 546-686K (273°-413°C). The temperature range which the exothermic peak spanned was approximately equal to that of the second endothermic peak.

The data from the traces of the two TMP variations were replotted to obtain a clearer representation of the reactions. The plot for the material processed by the heavy reduction schedule is presented in Figure 4.6. The data for the light reduction material is shown in Figure 4.7.

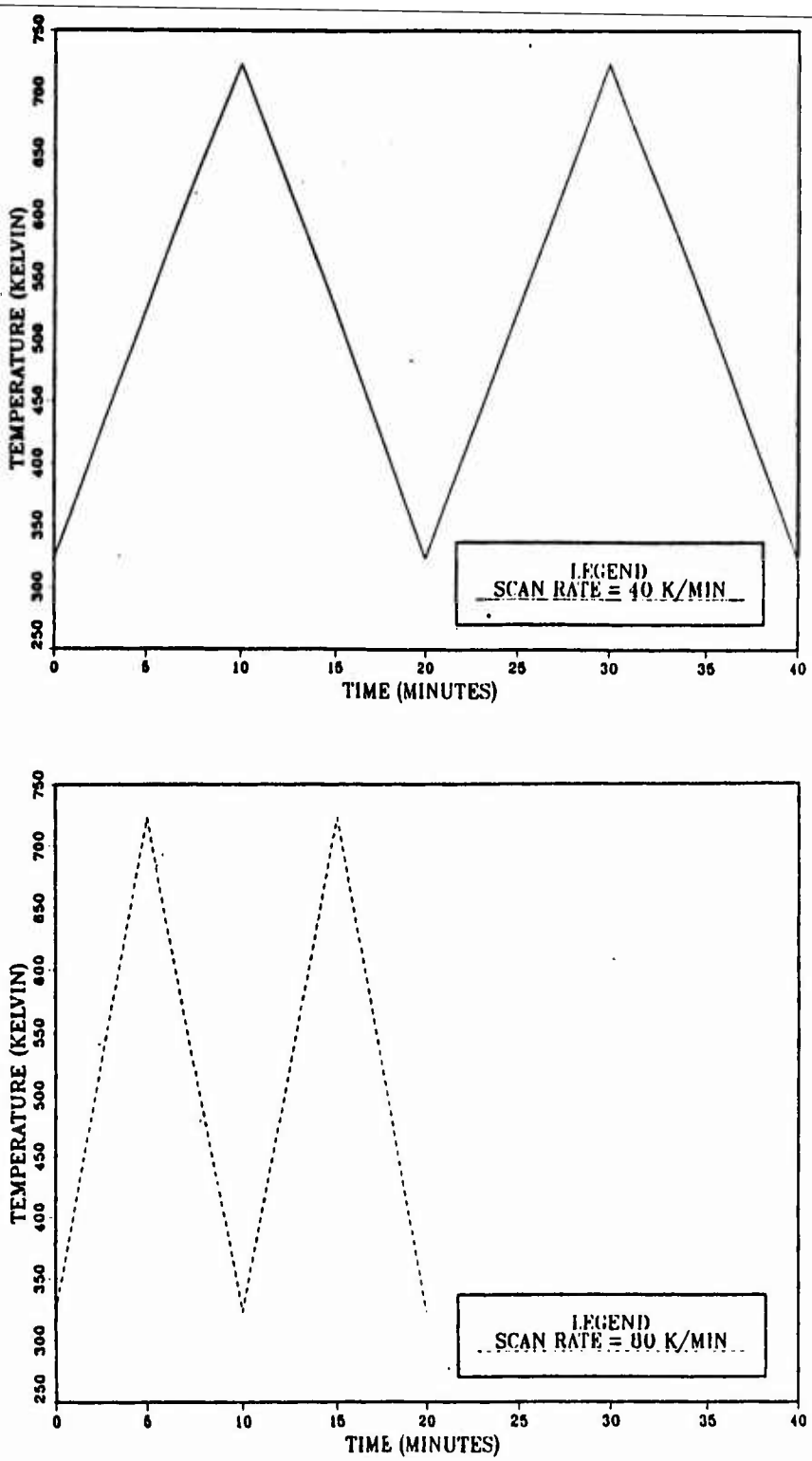

Figure 4.1 Schematic representation of the heating and cooling cycles.

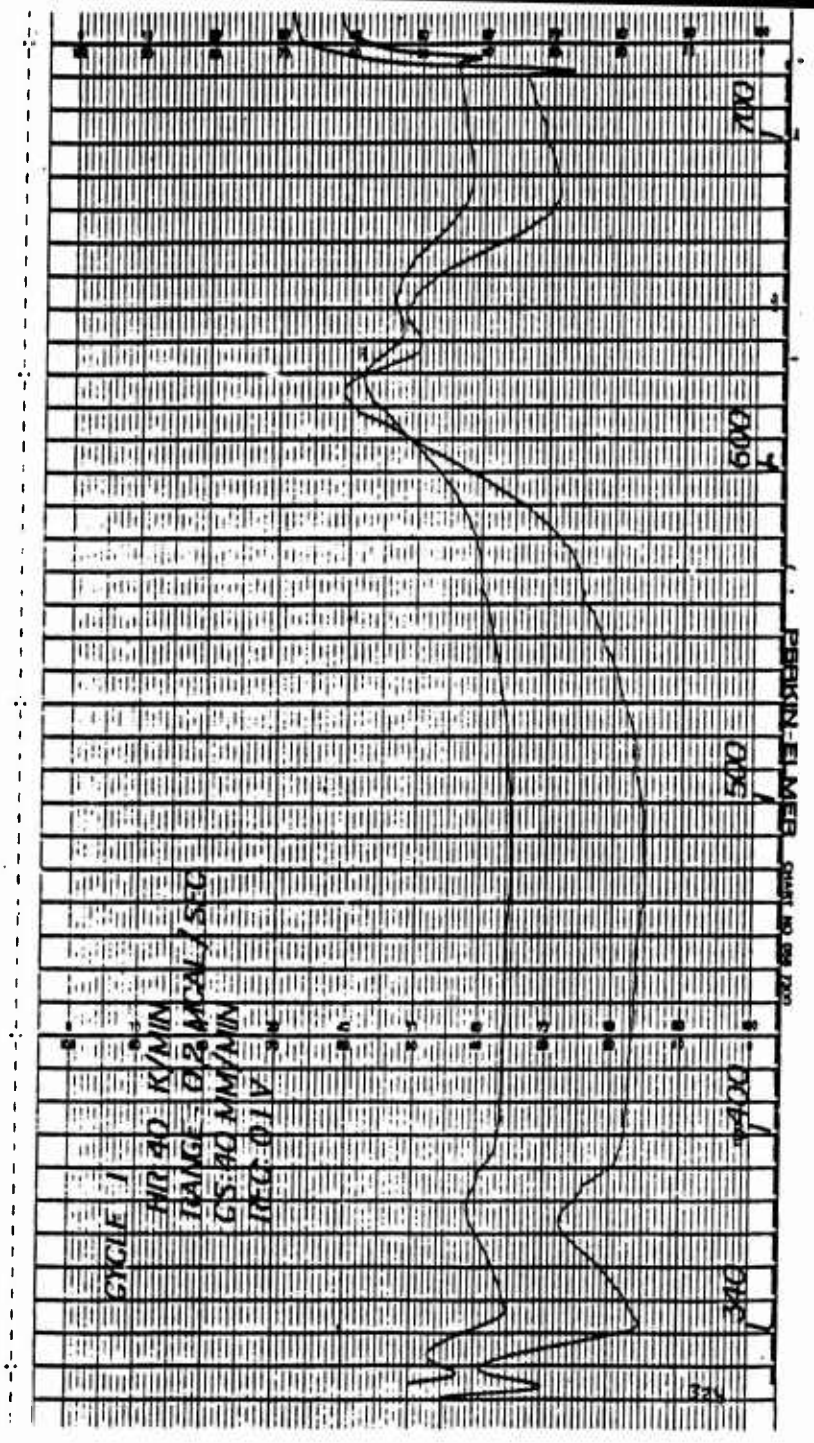

Figure 4.2 DSC trace of 1st heating scan of heavy reduction material. Scan rate = 40K/min.

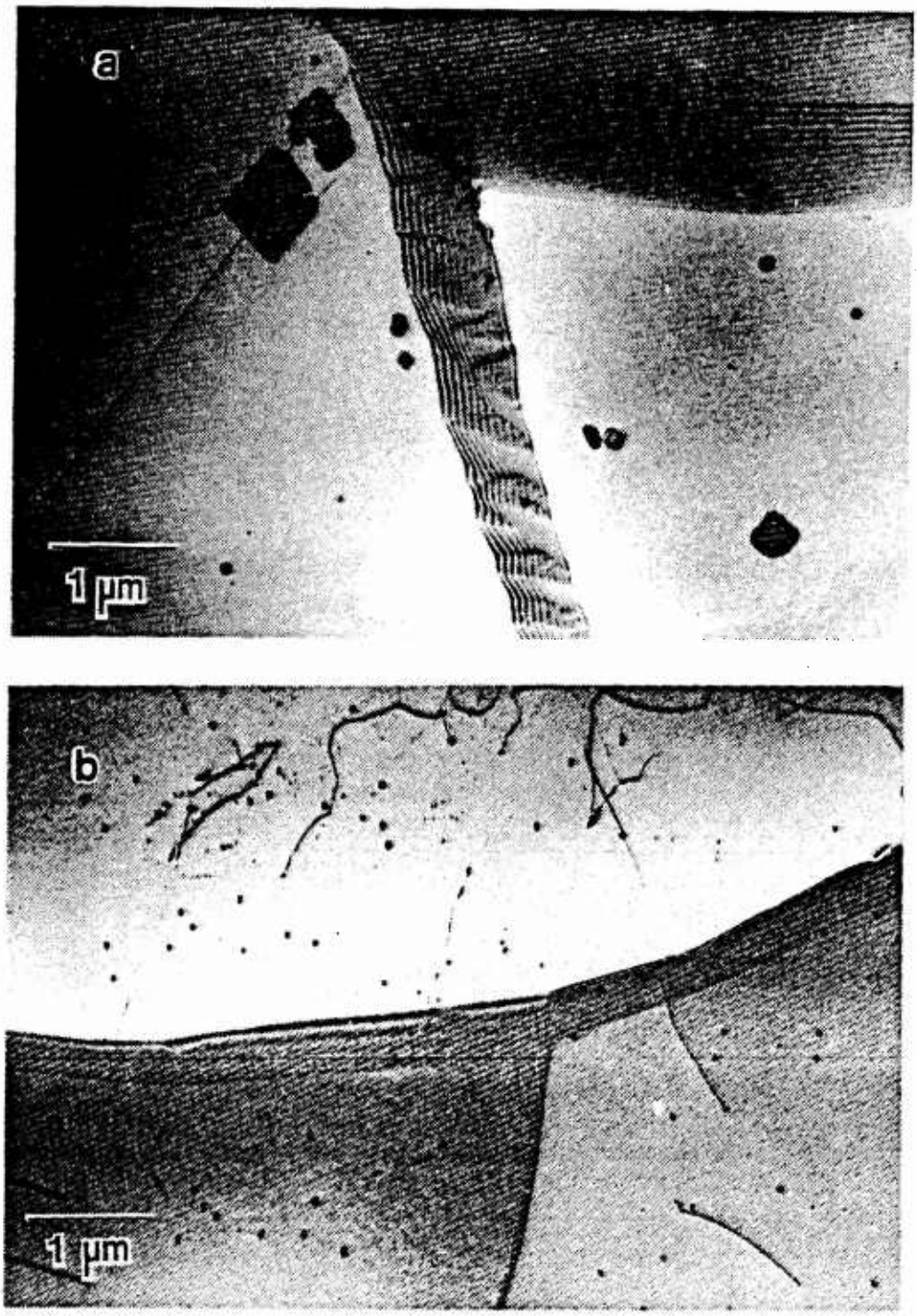

Figure 4.3 TEM micrograph of Al-10Mg-0.1Zr heated to 733K: (a) Heavy reduction material, (b) Light reduction material.

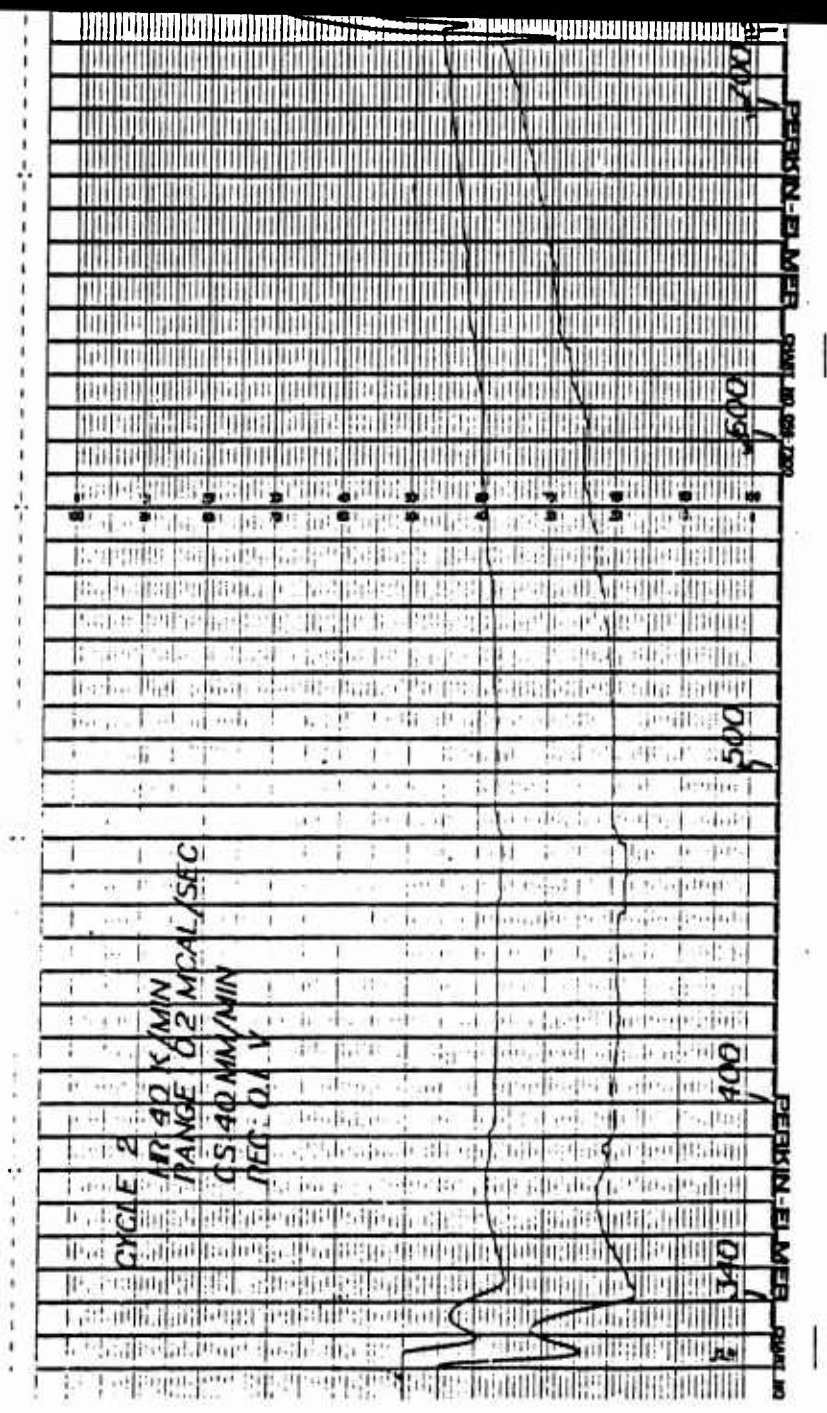

Figure 4.4 DSC trace of 2nd heating scan of heavy reduction material. Scan rate = 40K/min. Second scan of material shown in Figure 4.2.

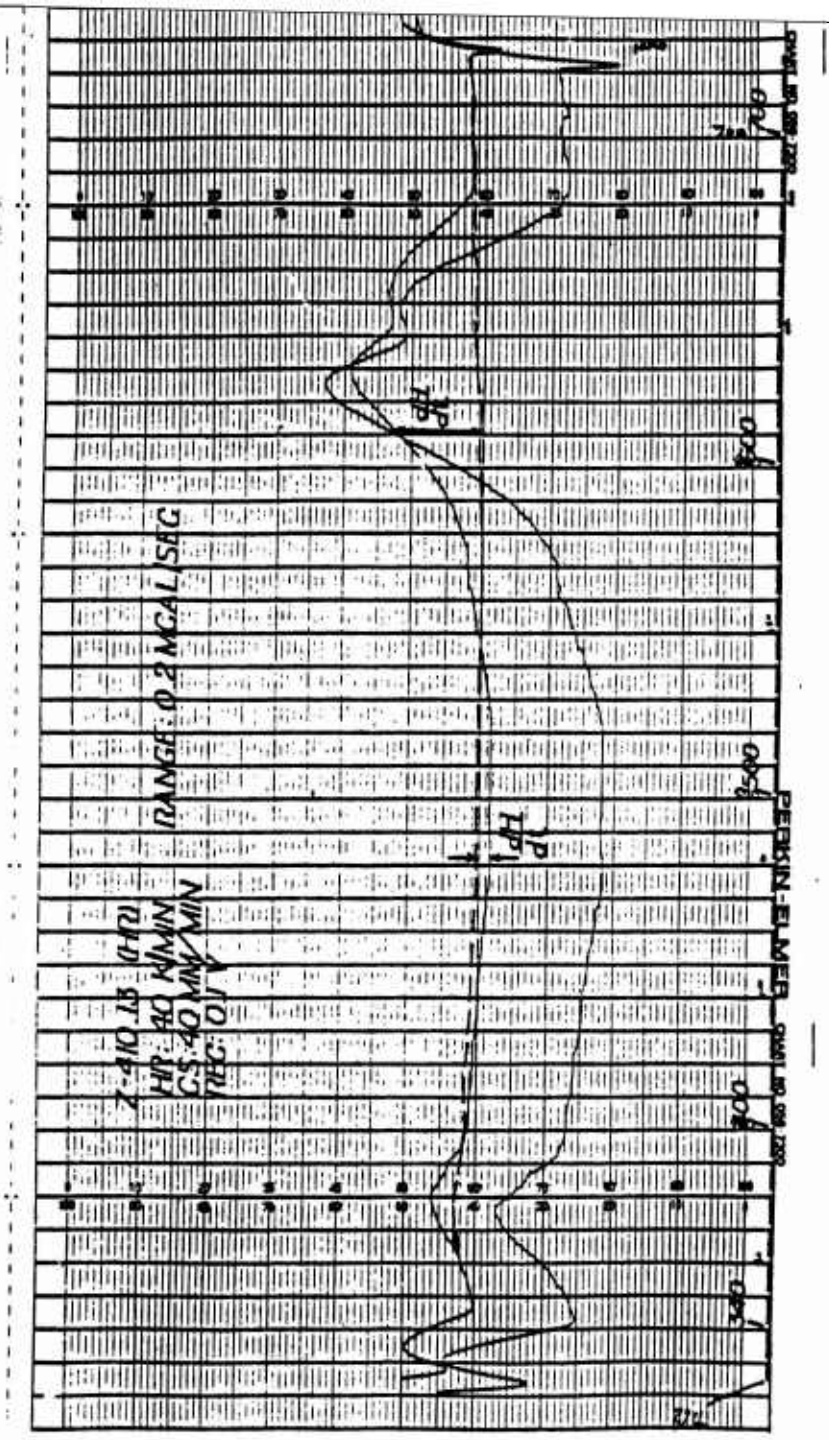

Figure 4.5 DSC trace of 2nd trace superimposed on 1st trace. dH/dt measured from baseline (2nd trace).

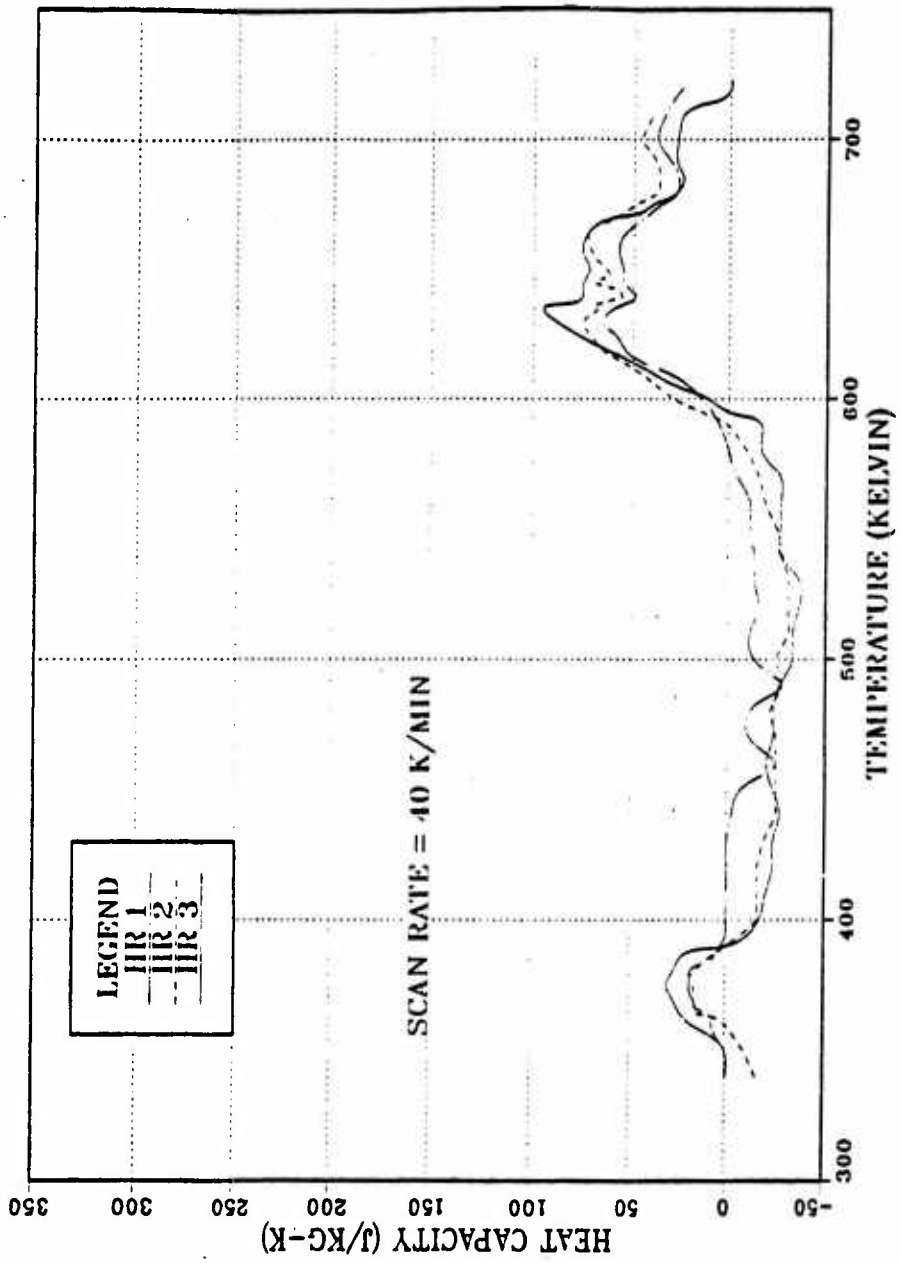

Figure 4.6 ΔC_p vs T plot for heavy reduction material. Scan rate = 40K/min.

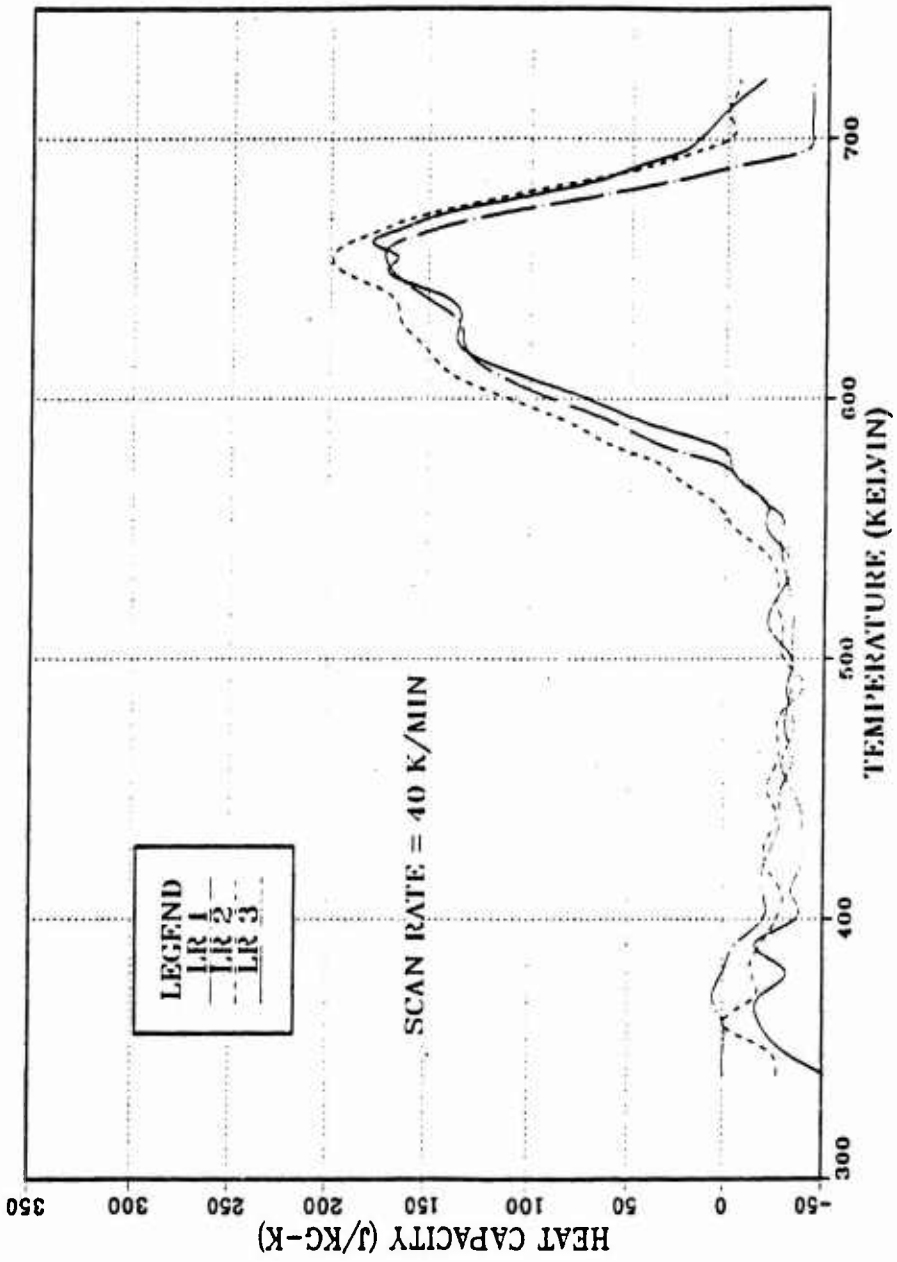

Figure 4.7 ΔC_p vs T plot for light reduction material. Scan rate = 40K/min.

B. DSC COMPARISON OF TMP VARIATIONS

1. Low Temperature Endotherm

The data from a representative DSC scan for each TMP variation was plotted to determine the effects of the different processing schemes. This information is displayed as Figure 4.8. As seen in this figure, a low temperature endothermic peak was readily distinguishable in the heavily reduced material, while an extremely small endothermic peak was visible in the more lightly rolled material. Both peaks occurred over approximately the same temperature range. The position and relative magnitude of the first endothermic peak corresponds to similar ones observed by Lendvai, *et al* [Ref. 25:p. 593], Lacom, *et al* [Ref. 26:p. 253], DeIasi and Adler [Refs. 27,28:pp. 225,762], and Papazian [Refs. 29,30:pp. 225,762]. In each case the lower temperature endothermic peak was associated with the dissolution of Guinier-Preston (GP) zones in other aluminum alloys. Osamura and Ogura [Ref. 31:p. 837] reported similarly the presence of GP zones and associated endotherm for an Al-Mg alloy. According to Mondolfo [Ref. 6:p. 316], GP zones are formed in the first few seconds following the quench. It is therefore reasonable to attribute the first endothermic peak to the dissolution of GP zones which formed when the sample was quenched after either hot working or warm rolling.

The aluminum magnesium alloy being investigated in this work does not obtain any additional strength from the formation of GP zones [Ref. 6:p.316]. Also the solid state reaction associated with the dissolution of GP zones occurs well below the temperatures of interest. Therefore the microstructural changes associated with the first endothermic peak were not pursued as a part of this study.

2. Exothermic Peak

A broad, shallow exothermic peak was exhibited by both processing variations. In each case the exotherm covered an approximate temperature range of 200K. The heat capacity magnitudes were nearly equal for both conditions and were relatively small in comparison to the second endothermic peak. Clarebrough *et al.* [Ref. 32:p. 98] observed exothermic activity in aluminum of 99.998% purity, deformed 75% in compression at room temperature, which was similar in shape and position to that shown in Figure 4.8. In the calorimetric studies of an Al-Mn alloy by Howe [Refs. 33,34:pp. 595,610] similar behavior was also observed. Both Clarebrough and Howe attributed the exothermic activity to recovery in the worked materials.

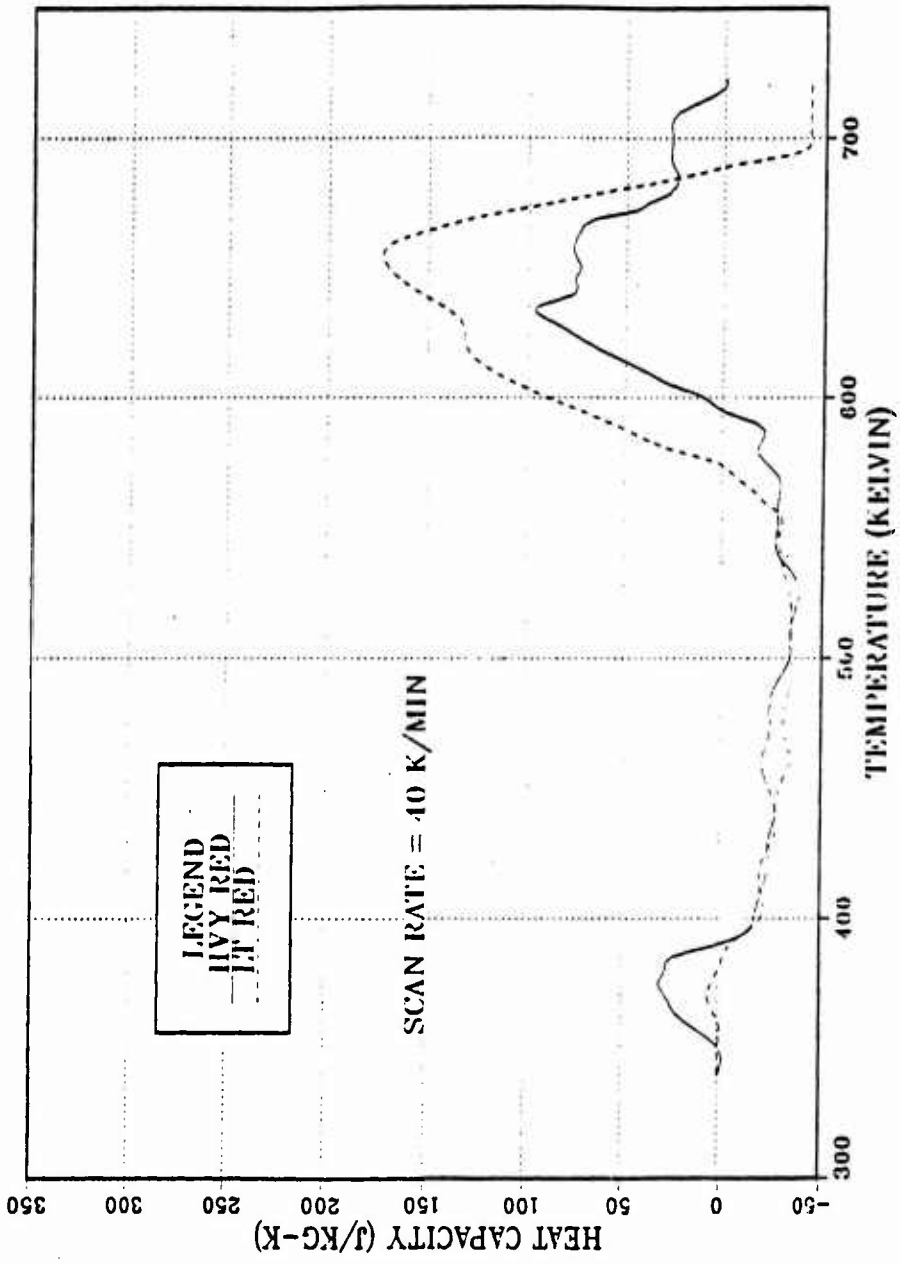

Figure 4.8 ΔC_p vs T plot comparison of heavy reduction and light reduction material.

3. High Temperature Endothermic Peak

A large endothermic peak was seen in both the heavy reduction material and the light reduction material. The temperature range spanned by these endotherms was approximately equal. The endotherm for the light reduction material appears to start and end about 25K before the heavy reduction material endotherm. The most notable differences between the two peaks were their basic shapes and magnitudes. On the heavy reduction material, a higher amplitude peak was registered first, followed by a lower level peak or plateau. The opposite situation was seen in the light reduction material with a lower amplitude peak occurring first followed by the peak of greater amplitude. Similar large endothermic peaks at the upper end of the temperature range scanned have been reported [Refs. 27,28,29,30:pp. 1178,1187,225,763] for various aluminum alloys. The dissolution of precipitates was the reaction causing the endotherm in those cases. Additionally, as seen in Figure 2.1, the solvus temperature for a nominal 10% Mg Al-Mg alloy, ~615K, lies within the temperature span of both endotherms.

Based on the immediately preceding discussion, the difference in the shape and magnitude of the endothermic peaks resulted from the dissolution of the β precipitate. Grider [Ref. 20:pp. 37,41] noted that the size and distribution of β phase varied with the reduction schedule used. Material processed by the light reduction schedule contained a uniform distribution of relatively coarse β phase, while the heavy reduction material was found to have a less uniform distribution of finer β phase particles. In addition, the TEM micrographs of the as-rolled materials, Figure 4.9, has shown the β phase precipitated on grain boundaries of the light reduction material to be coarse and and more nearly discontinuous. The β phase in the heavy reduction was a finer, but more continuous grain boundary film. The difference in the morphology of the β phases of the two TMP variations may possibly account for the dissimilarity between the two endothermic peaks.

C. MICROSTRUCTURAL EVOLUTION DURING HEATING

Differential scanning calorimetry provided suggestions for the sequence of the microstructural evolution in the alloy being studied. However, that analysis alone is insufficient to characterize accurately and completely the changes in the microstructure. To observe the evolution, transmission electron microscopy was utilized. Based on the DSC data, three temperatures of significant interest were selected:

1) the end of the exothermic peak, ~563K (290°C)

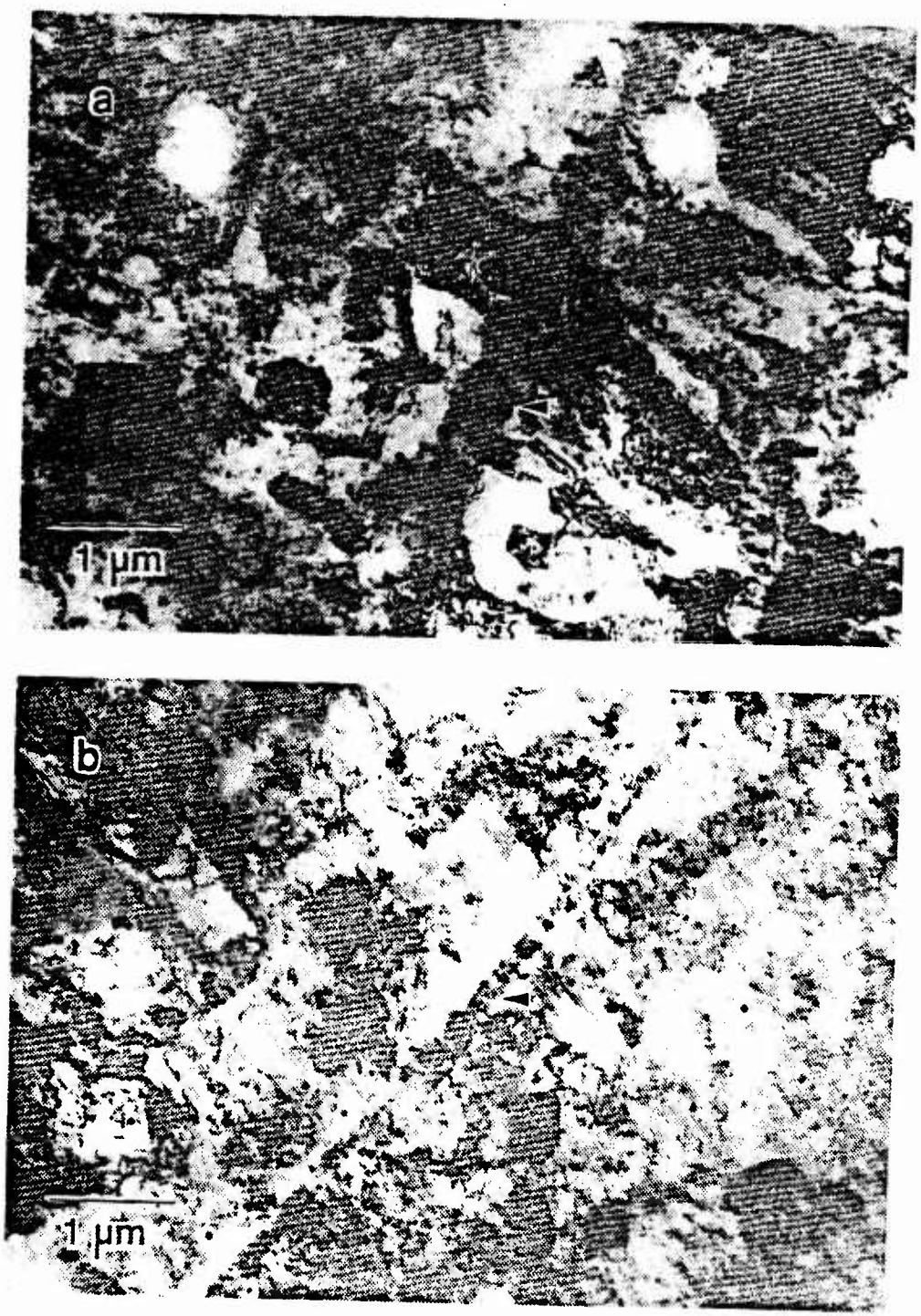

Figure 4.9 TEM micrograph of Al-10Mg-0.1Zr in as rolled condition: (a) Light reduction, (b) Heavy reduction. Arrows indicate β on prior grain boundary.

2) the saddle point in the higher temperature endotherm, ~633K (360°C)

3) the upper end of the temperature range, 723K (450°C)

Upon attaining those temperatures in the DSC, the samples were rapidly cooled as shown schematically in Figure 4.10. The samples were then examined in the transmission electron microscope.

1. **Initial Microstructure**

The microstructures for the as rolled condition for the two TMP variations were essentially identical. A heavily distorted matrix with high dislocation density tangles was exhibited by both the heavy reduction and the light reduction materials, as shown in Figure 4.9. No apparent grain structure could be discerned, and the substructure was disorganized. Intermetallic β phase precipitated in grain interiors and as a nearly continuous film on what appeared to be prior grain boundaries. In a similar Al-Mg alloy, McNelley and Garg [Ref. 24:p. 918] noted an approximate volume fraction of 10% for the β. The β was generally submicron in size. As previously noted, the grain boundary β in the heavy reduction material was more obvious and varied in width from 160-265 nm. In the light reduction material, the β precipitation was coarser and less regular on the grain boundary. Widths of the β in the light reduction material varied from 380-790 nm. These differences are evident in Figure 4.9.

A microstructure of this type is not expected to exhibit superplastic behavior according to current theory. However, superplastic response of this alloy has been obtained at NPS by Hartman [Ref. 35], Berthold [Ref. 36], Klankowski [Ref. 23], and Grider [Ref. 20]. It can therefore be concluded that at some point prior to or during the deformation of the as rolled material, the microstructures have evolved to ones which are capable of accommodating superplastic deformation.

2. **Microstructure at 563K (290°C)**

The microstructure attained upon heating the heavy reduction material to 563K is shown in Figure 4.11. The microstructure for the light reduction material is seen in Figure 4.12. Although the microstructures for both conditions still comprise a distorted matrix with a relatively high dislocation density, the most obvious change from the as rolled condition was the onset of a substructure formation. The dislocations have begun to arrange themselves into dislocation walls surrounding small, relatively dislocation-free regions. These regions are generally submicron in size. The light reduction material appeared to have a lower dislocation density at this temperature than the heavy reduction material, consistent with the greater time at

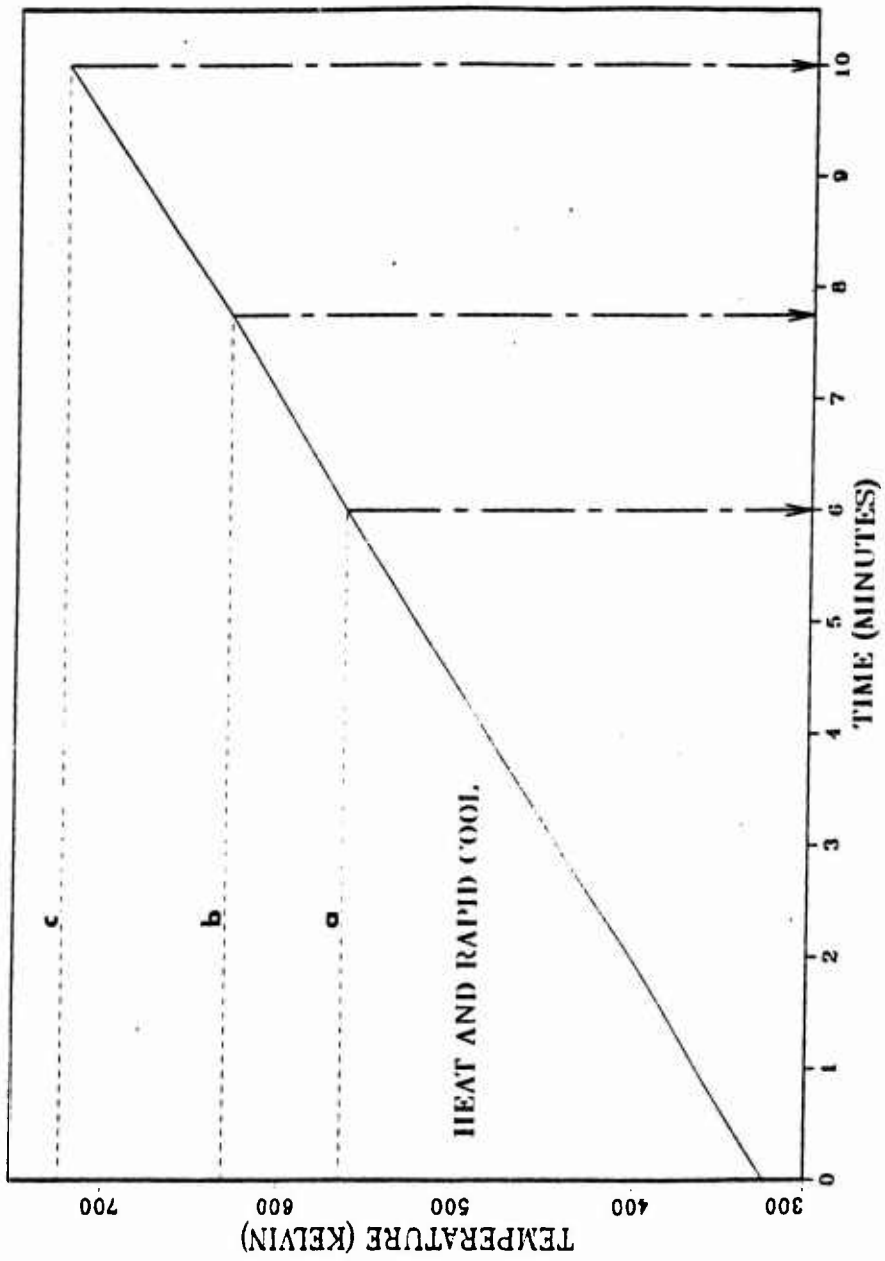

Figure 4.10 Schematic of DSC scans to selected temperatures: (a) 563K, (b) 633K, and (c) 723K).

temperature during warm rolling. This local rearrangement of dislocations to form a cell structure results in the release of energy as a lower energy configuration is attained [Ref. 15:p. 192]. The exothermic peak seen in Figure 4.8 can thus be attributed to the recovery of the warm worked structure which took place in the six minutes required to heat the sample from 323K to 563K (50°-290°C). Previous research at NPS [Ref. 37:p. 1276] has shown that material subjected to similar thermomechanical processing and held at 573K (300°C) prior to tension testing produced a recrystallized grain structure capable of supporting superplastic deformation.

In both TMP variations heated to 563K, the β phase was still present in abundance, with particle sizes of 1.0-1.8 μm in the light reduction material and 0.2-0.6 μm in the heavy reduction material. The size difference in the β most likely reflects the size difference seen in the as rolled microstructures. A prior grain boundary on which β had precipitated was located in the heavy reduction material, and the precipitate size had increased to widths of 300-700 nm. No prior grain boundaries were found in the lightly reduced material.

The light reduction material exhibited a few isolated regions which appeared to be the nucleation sites for discontinuous recrystallization. Although found only rarely in the foils, every case examined was adjacent to a β particle approximately 1.0 μm in size. Similar areas were not found in the heavy reduction material.

3. **Microstructure at 633K (360°C)**

Upon heating to 633K, more extensive changes have taken place in the microstructures of both TMP variations. These changes are reflected in the TEM micrographs for both the heavy reduction and the light reduction materials, Figures 4.13 and 4.14, respectively. Both materials have continued to undergo recovery, but now, extensive recrystallization has also occurred. Large dislocation-free grains (15-50 μm in the light reduction material and up to 250 μm in the heavy reduction material) were apparently formed by a nucleation and growth, or discontinuous, process of recrystallization. Some of the grains are associated with intergranular β particles, as shown in Figure 4.14, which appear to have acted as nucleation sites. Other recrystallized grains have apparently swept through and eliminated regions in varying stages of recovery and have been halted by arrays of β which had precipitated on grain boundaries during the prior warm rolling. Figure 4.13 shows a recrystallized region separated by intergranular β from a region containing a recovered structure. For the lightly reduced material, approximately 95% of the TEM foil area had

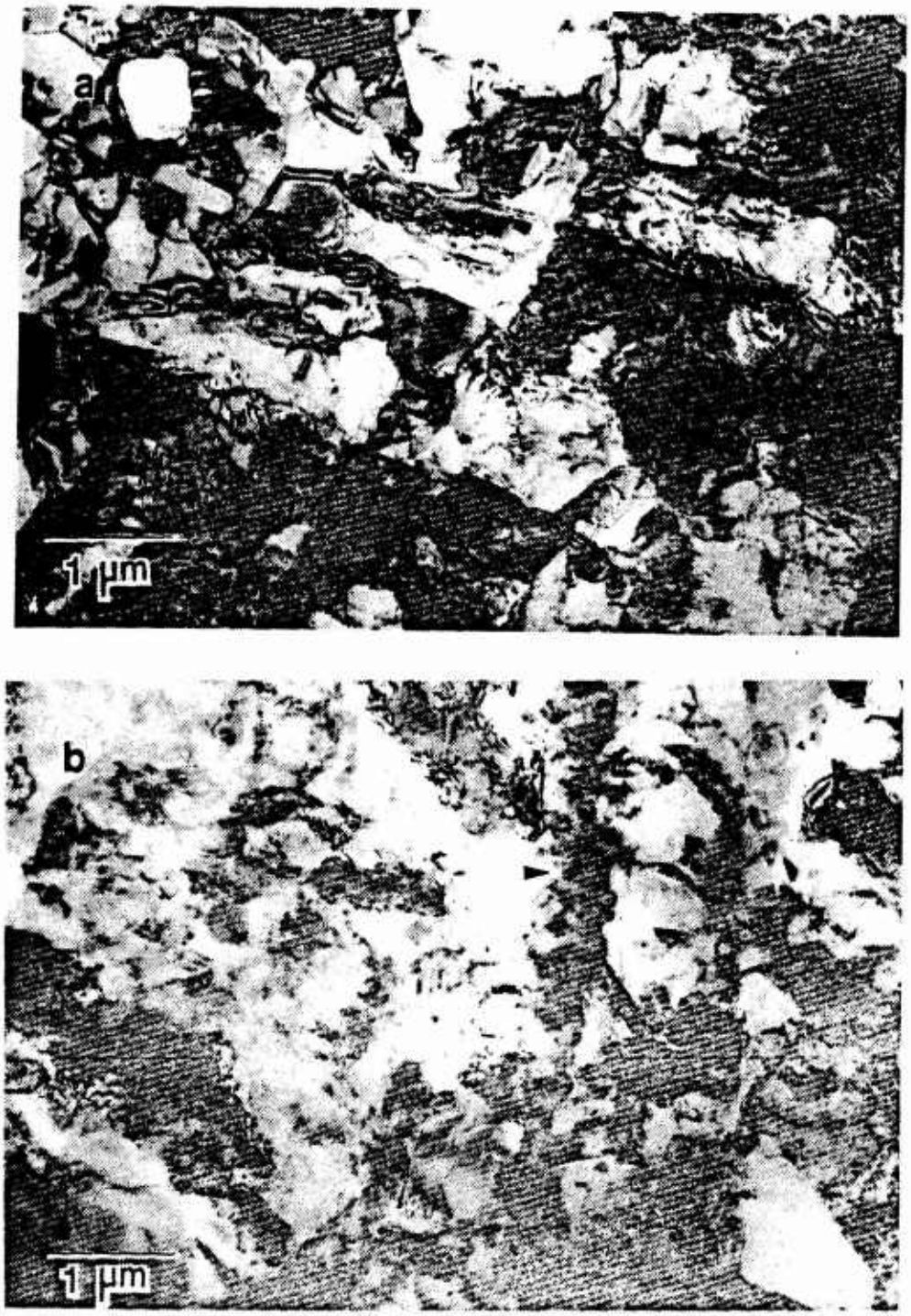

Figure 4.11 TEM micrograph of heavy reduction Al-10Mg-0.1Zr 563K scan: (a) Partially recovered region, (b) β on prior grain boundary.

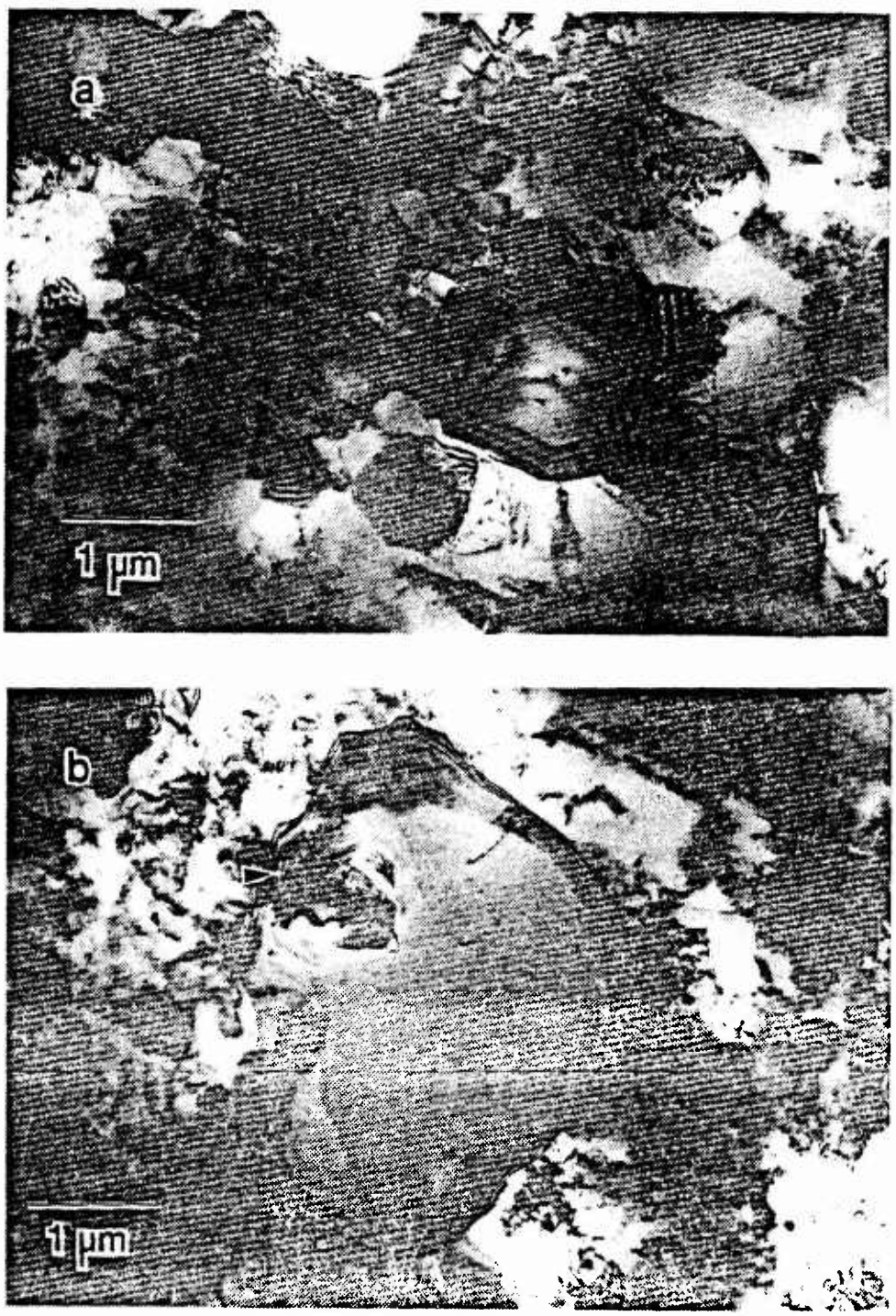

Figure 4.12 TEM micrograph of light reduction Al-10Mg-0.1Zr 563K scan:
(a) Partially recovered region,
(b) β nucleation site for discontinuous recrystallization.

recrystallized discontinuously with the remaining area in various stages of recovery. Recrystallization by nucleation and growth had also occurred in the heavy reduction material, but to a lesser extent. Approximately 50% of the foils of the heavily reduced material had discontinuously recrystallized. As with the light reduction schedule, areas which had recovered to form a fine substructure, 1-4 μm in size, were adjacent to the recrystallized regions. The degree of freedom from dislocations in the recovered regions varied from an almost total absence, Figure 4.13, to a stage just slightly advanced beyond that found in the 563K condition, Figure 4.14.

Previous research by Grider [Ref. 20:pp. 37,41] indicated that the size and distribution of the β was not identical in the as rolled material of the two TMP variations. The size difference was also noticable when the materials were heated to 563K. As a result of the coarser β providing a greater number of favorable nucleation sites, i.e. particles larger than 1 μm in diameter [Ref. 38:p. 391], the light reduction samples began to recrystallize at a lower temperature than the heavy reduction material. Recrystallization likely was delayed in the heavy reduction material until the β coarsened to a critical size required to act as a nucleation site. The size of the largest β particle observed increased from 0.6 μm to 1.1 μm as the material was heated to 633K. The earlier onset of recrystallization in the light reduction material accounts for the greater percentage of recrystallized area.

Examination of the microstructure heated to 633K was done to determine the cause of the endothermic activity seen on the DSC trace. It was thought that the endotherm reflected dissolution of β, which should have been evidenced by reduced volume fraction and particle size of β. The micrographs, however, do not show any β size decrease. In the case of the heavy reduction the β increased to 0.6-1.1 μm, and the light reduction β size remained relatively constant at 0.8-2.0 μm. It cannot be conclusively stated from this study that the β phase has begun to dissolve at 633K, even though the material was at or above the solvus temperature. To assess more accurately the quantity of β present at 633K it would be necessary to make volume fraction measurements. Time constraints and the requirements for statistical accuracy prevented those measurements from being made. The presence of the endotherm in DSC results for both TMP variations presents a strong case for expecting that dissolution of β has occurred up to this temperature.

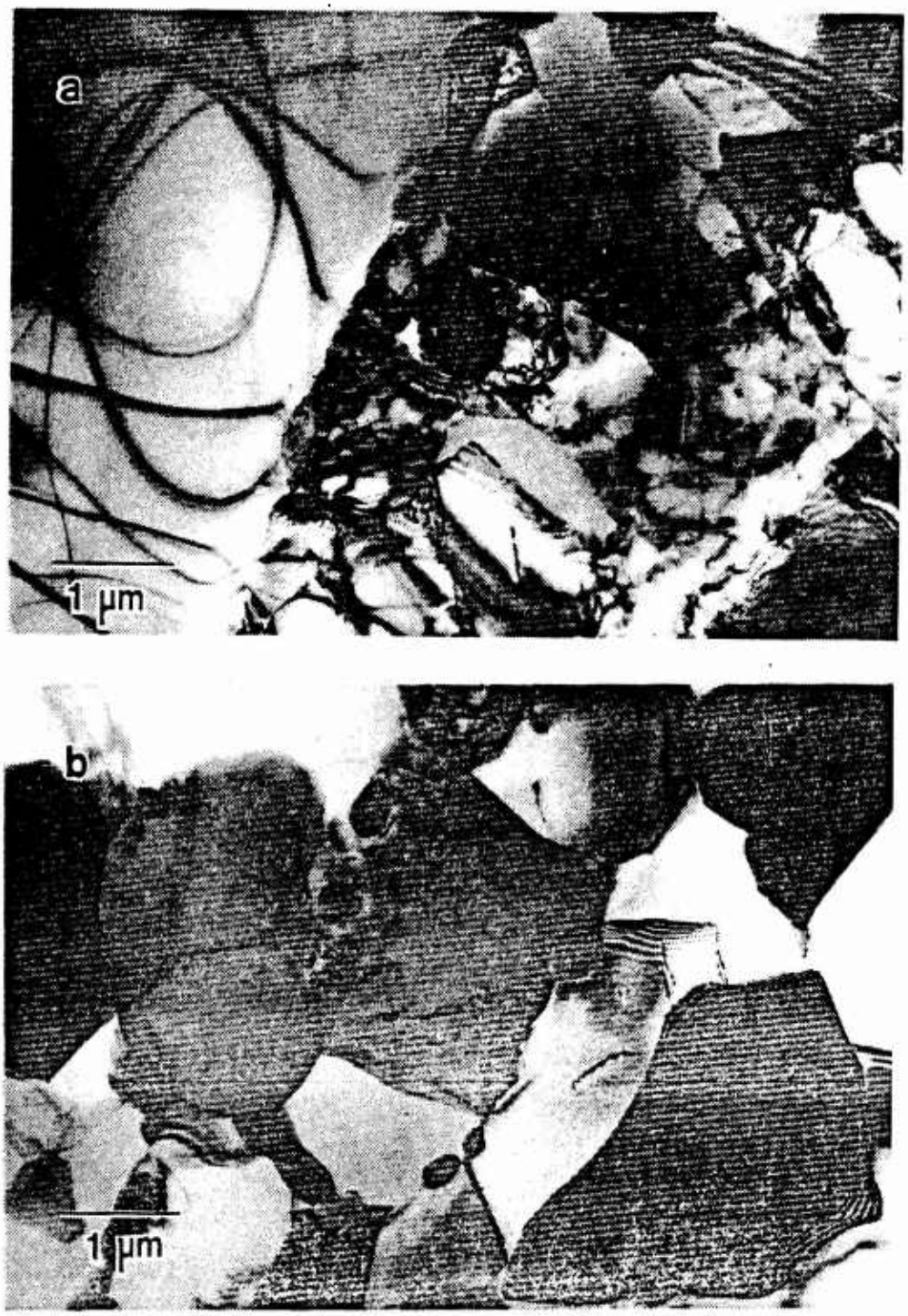

Figure 4.13 TEM micrograph of heavy reduction Al-10Mg-0.1Zr 633K scan: (a) Discontinuously recrystallized grains separated by β from recovered region (b) Recovered region.

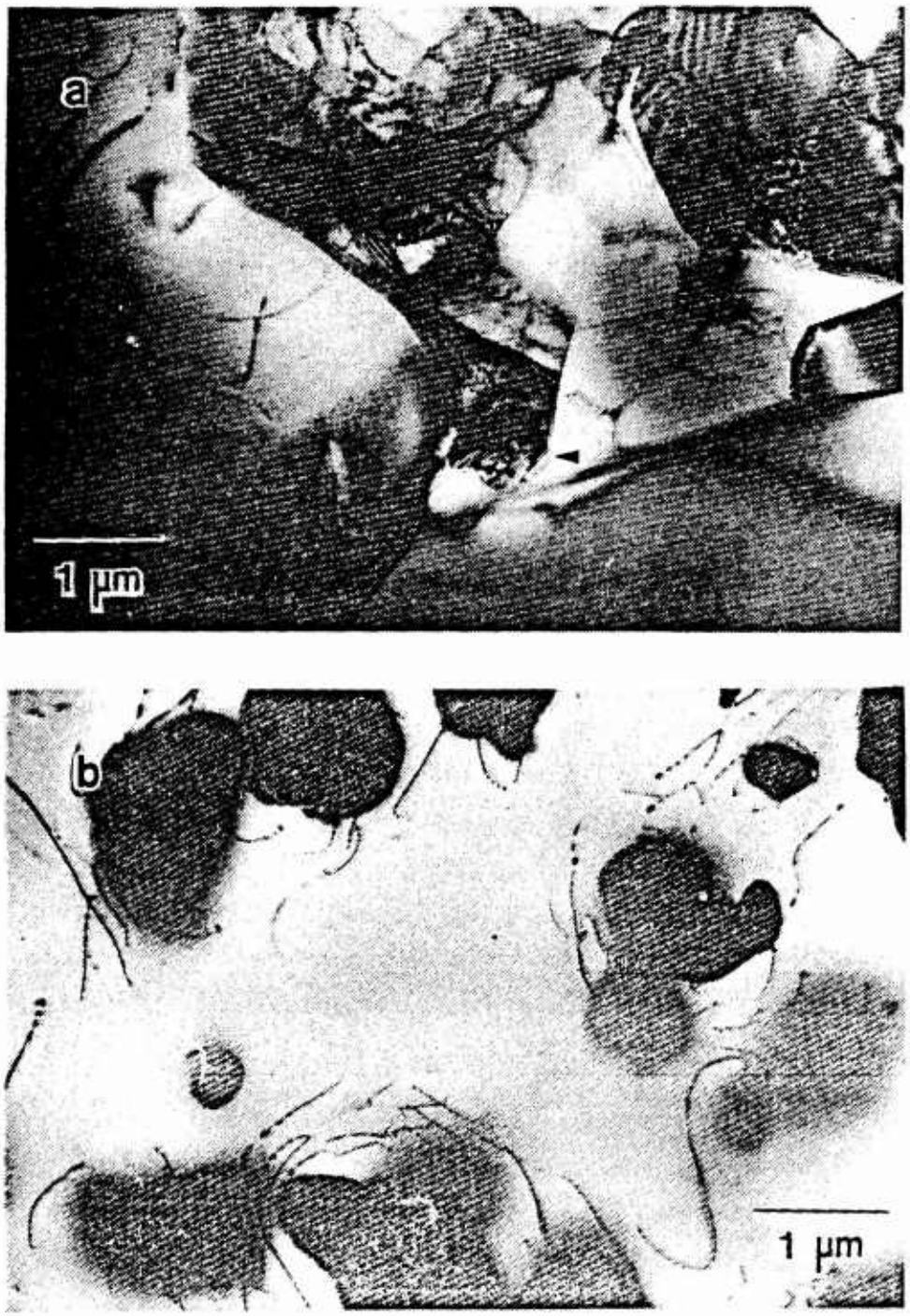

Figure 4.14 TEM micrograph of light reduction Al-10Mg-0.1Zr 633Kscan:
(a) Discontinuously recrystallized grains nucleated at β
(b) β in recrystallized grain interiors.

4. **Microstructure at 723K (450°C)**

At the upper end of the temperature range, the microstructures of both TMP variations were fully recrystallized, as seen in Figure 4.3 and Figure 4.15 . The light reduction material exhibited a grain structure of almost exactly the same size, 10-50 μm, as seen at 633K. Grain interiors wered completely free of the dislocation tangles introduced during the warm rolling. Grains in the heavy reduction material had increased in size and were an order of magnitude larger than those of the lightly reduced material, reaching a maximum size of 500 μm. Both the heavy and light reduction material contained some dislocations which are believed to have formed during the rapid cooling of the samples. The grain size of the light reduction material was limited by the nucleation of a large number of grains by the β at lower temperatures. Greater grain growth occurred in the heavy reduction material due to the retention of dislocations and a lesser number of nucleation sites. As the heavy reduction material was heated above 633K, sufficient driving force existed to result in further recrystallization and grain growth. The β previously observed in the grain interiors and on prior grain boundaries was completely absent in the heavily reduced sample after heating to 723K. No β was seen in the grain interiors of the light reduction material. Some extremely fine β, 500-600 nm in width, was seen at a prior grain boundary, most likely the undissolved remnants from precipitation at a prior grain boundary. The short time of the heating cycle, ten minutes, combined with the rapid cooling upon reaching 723K may have precluded the dissolution of the coarse β precipitates on the grain boundaries. The complete recrystallization of the microstructures and dissolution of β phase at 723K agreed with the DSC data which indicated a return to baseline values indicating a stop of solid state reactions.

D. MICROSTRUCTURAL CHARACTERIZATION OF ANNEALED ALLOY

As a means of comparing and further defining the microstructural evolution seen in the two thermomechanical processing variations, a sample of Al-10.0%Mg-0.1%Zr alloy from previous work [Ref. 23] was examined in the DSC and by TEM. The material was processed by the light reduction schedule and was then annealed for 1.5 hours at 573K (300°C). The micrograph of the annealed condition, Figure 4.16, shows that a well-defined structure had formed encompassing dislocation-free regions. Thus it appears to be a recrystallized structure with a fine grain size. This conclusion is based in part upon the 300-500% elongations obtained from the structure when the alloy was

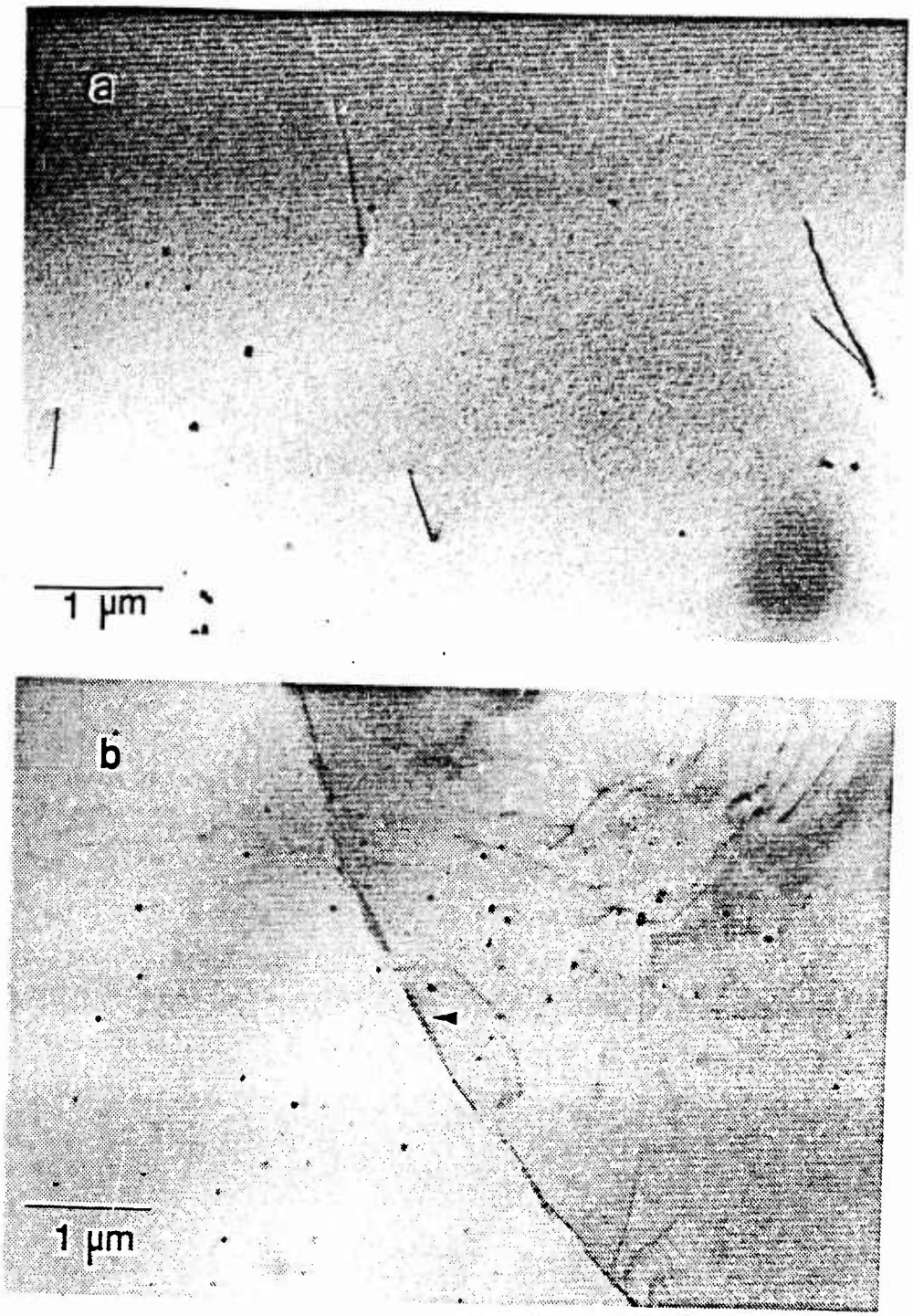

Figure 4.15 TEM micrograph of Al-10Mg-0.1Zr 723K scan:
(a) Heavy reduction - recrystallized grain interior
(b) Light reduction - β remnants from prior grain boundary.

tension tested at 573K [Refs. 35,39:pp. 48,74]. When a fully recrystallized sample, obtained by heating to 713K, was tested under identical conditions [Ref. 36:p. 74], a superplastic response was not obtained.

The light reduction and 573K annealed material was examined by differential scanning calorimetry as the previous material had been. The results produced by the DSC are shown in Figure 4.17. The DSC plots for all three conditions are shown in Figure 4.18. No peaks were observed until the temperature reached approximately 523K (250°C). An exothermic peak, as observed in both the light and heavy reduction materials, was not expected since the 1.5 hours at 573K appeared from the microscopy to be sufficient for recovery and recrystallization. Any further heating of the material in the DSC would likely only produce some grain growth. The microstructure at 563K, Figure 4.16, shows no perceptible difference from the initial microstructure. The β precipitates observed were nominally 0.8-1.8 μm in size.

Continued heating of the annealed material produced an extremely large endothermic peak, twice the magnitude of the light reduction material. The peak covers approximately the same temperature range spanned by both the heavy and light reduction materials. The initial warm rolling of this material should have produced the same amount of β precipitation [Ref. 24:p. 918] as previously seen. Therefore the greater exothermic peak height cannot be the result of the dissolution of an increased amount of β. This was partially substantiated by the decreased β size (0.4-1.5 μm) seen in the micrograph for the annealed material at 633K, Figure 4.19. Previous data revealed discontinuous recrystallization had occurred in both TMP variations at this temperature. If it was assumed that the microstructure of the annealed material was completely recrystallized prior to heating to 633K, then no further recrystallization, and simultaneous release of energy, would be expected. The only subsequent change to the microstructure would be from grain growth which releases much less energy than recovery or recrystallization [Ref. 15:p. 192]. Therefore the DSC deflection corresponding to grain growth should be very weakly exothermic. The microstructure at 723K, consisting of 10-50 μm grains, is shown in Figure 4.19. From the preceding it was assumed that the endotherm for the annealed material can be used as the "pure" endothermic reaction exhibited during the dissolution of the β precipitates. Furthermore, the reduced magnitudes of the endothermic peaks for the heavy reduction and light reduction materials indicate a superposition of the endothermic reaction of β dissolution and the exothermic reaction of discontinuous recrystallization. In other

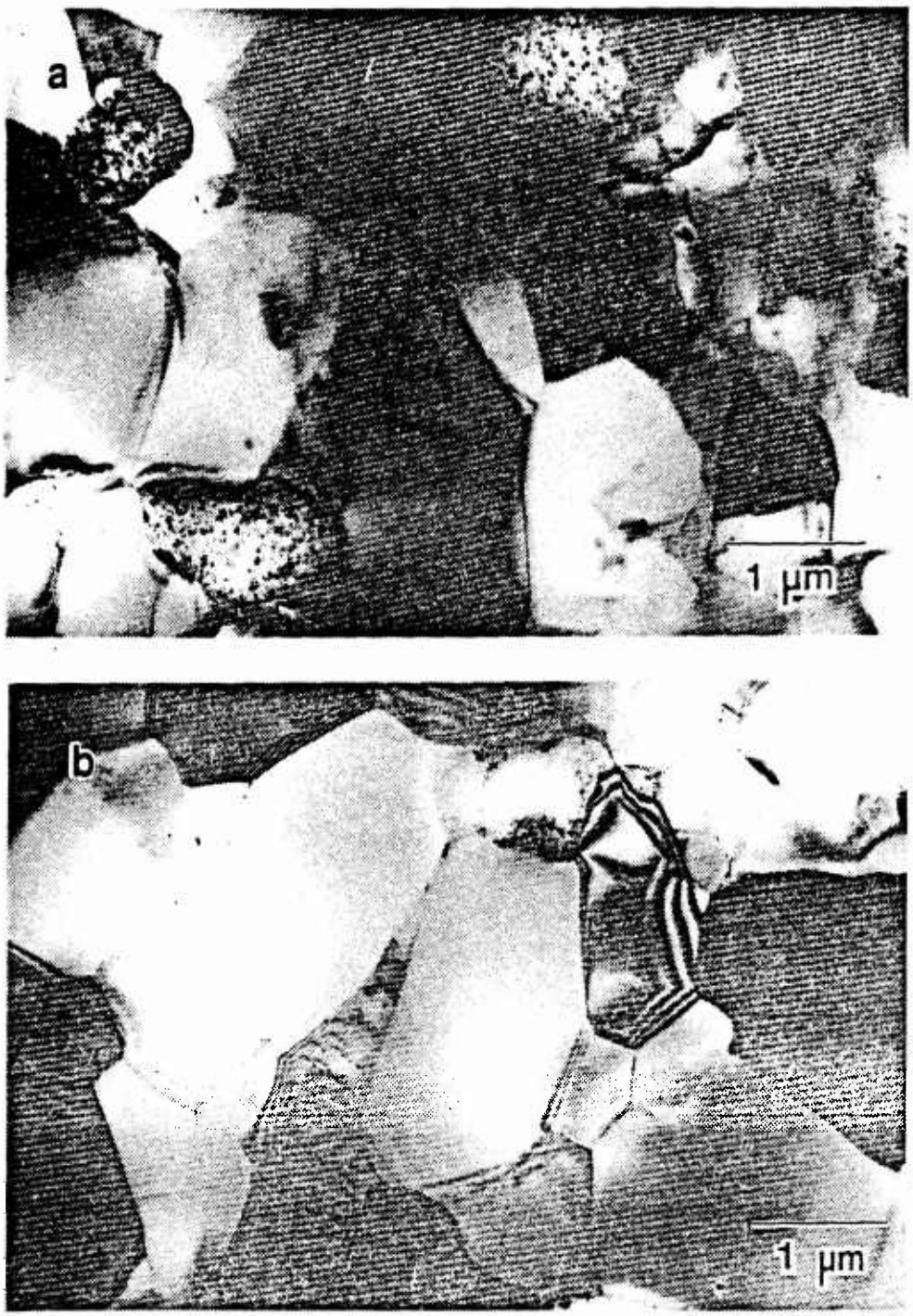

Figure 4.16 TEM micrograph of light reduction Al-10Mg-0.1Zr annealed for 1.5 hrs at 573K:(a) As annealed condition
(b) Heated to 563K and cooled to 295K.

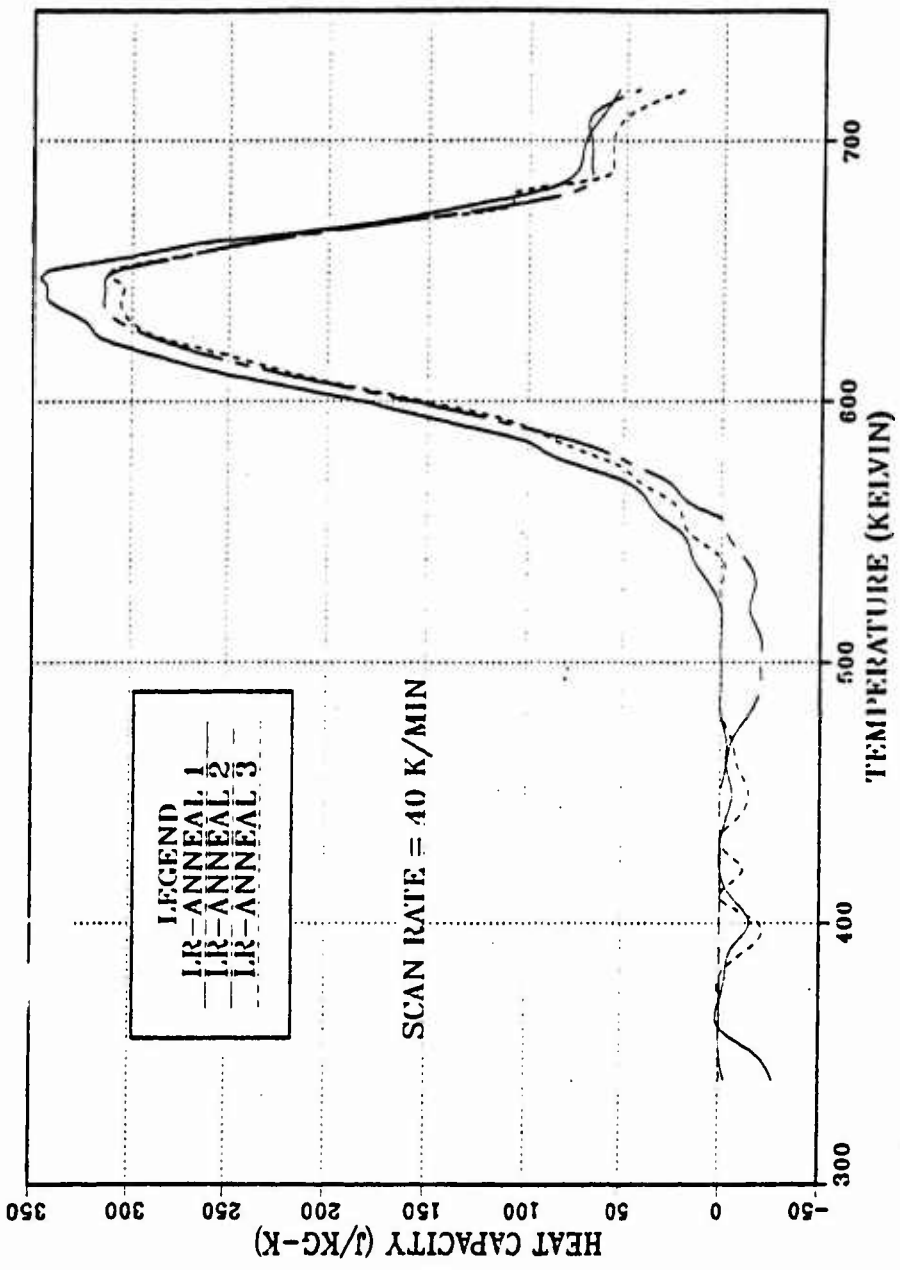

Figure 4.17 ΔC_p vs T plot of light reduction material annealed for 1.5 hrs at 573K.

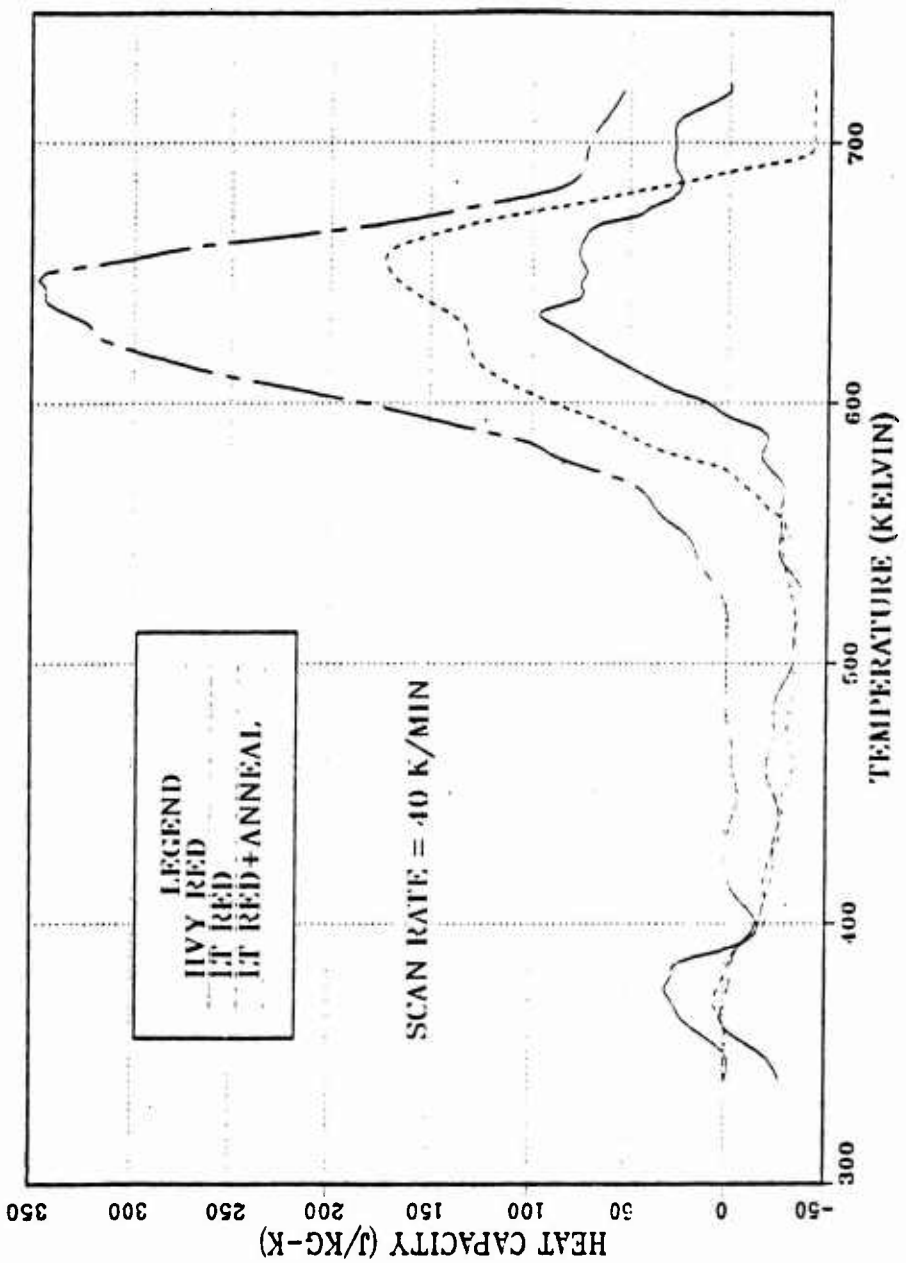

Figure 4.18 ΔC_p vs T plot comparison ofheavy reduction, light reduction, and light reduction and annealed materials.

aluminum alloys, similar superposition of endothermic and exothermic reactions [Ref. 29:p. 226] has been found.

As previously seen, the time spent at the rolling temperature for the heavy reduction material was relatively short. This reduced the opportunity for dislocation rearrangement and energy release during warm rolling, thereby creating a larger potential driving force for recrystallization that material. The lightly reduced material would have a lesser driving force due to the longer time at the warm rolling temperature. Upon recrystallizing the heavy reduction would have a greater amount of energy to release resulting in the smaller endothermic peak seen. The total reaction in the light reduction would produce a more pronounced endotherm due to the lesser stored energy.

E. IMPLICATIONS

There exists a small temperature range where, as a result of prior thermomechanical processing and annealing, a 1-5 μm grain size can be obtained by continuous recrystallization in this and possibly other alloys. The microstructural evolution would be controlled by the rolling and annealing treatments to produce material capable of being superplastically formed at relatively low temperatures, without cavitation, and to provide fine-grained material for enhanced corrosion and fatigue resistance.

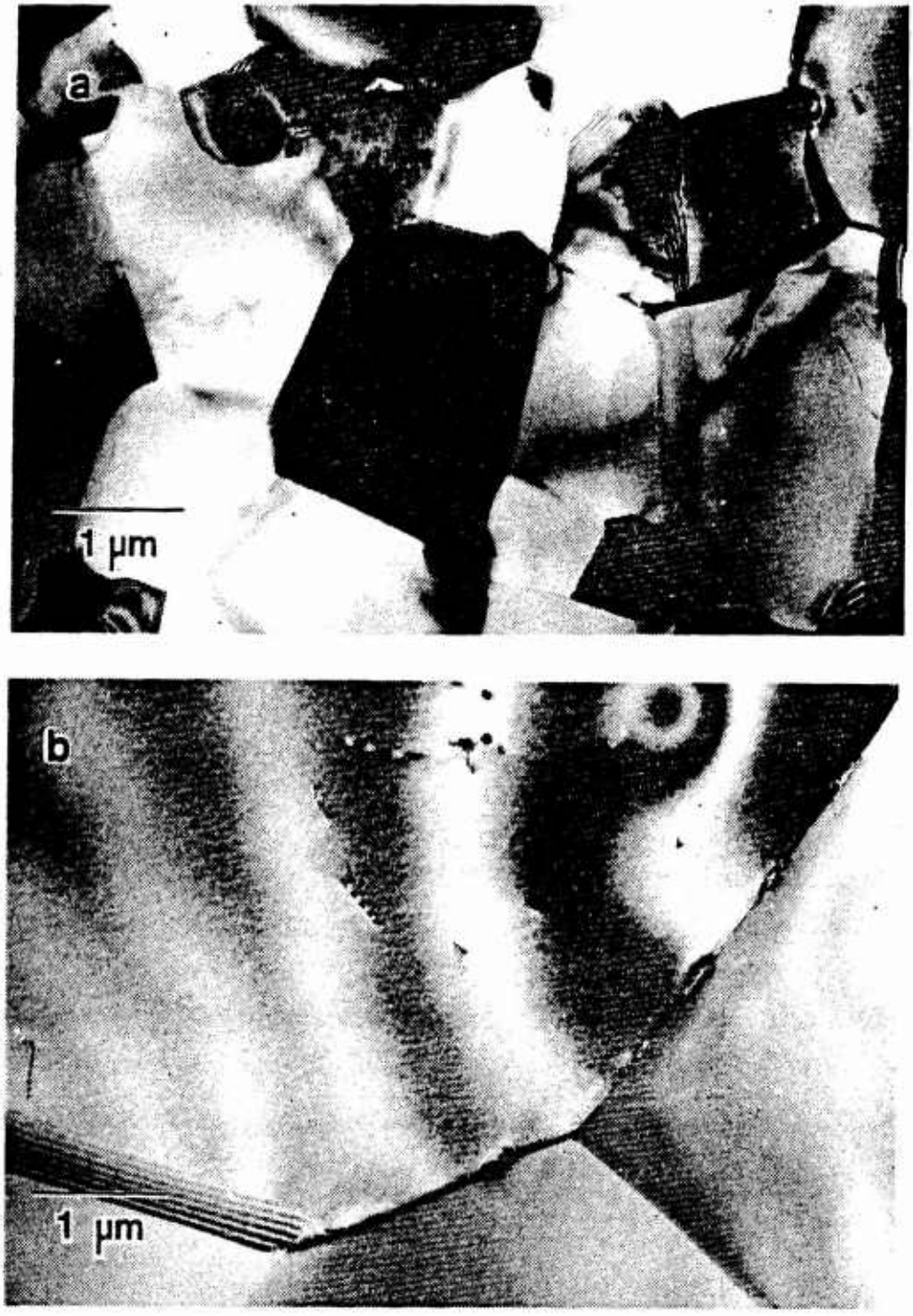

Figure 4.19 TEM micrographs of lightly reduced and annealed for 1.5 hrs at 573K:
(a) Heated to 633K and cooled to 295K
(b) Heated to 723K and cooled to 295K.

V. CONCLUSIONS AND RECOMMENDATIONS

The following conclusions have been drawn from the data presented in the previous chapters:

1. Differential scanning calorimetry is sensitive to the reactions of recovery, recrystallization and precipitate dissolutions which occur in this thermomechanically processed Al-Mg-Zr alloy.
2. The recovery of the highly deformed Al-Mg-Zr alloy starts after exposure to relatively low temperatures in a short time period.
3. Thermomechanically processed Al-Mg-Zr alloys have experienced some degree of recovery upon heating to 563K (290°C) in the DSC. This is a precursor to continuous recrystallization required to provide a fine-grained structure capable of supporting superplastic deformation.
4. Recrystallization by nucleation and growth has predominated the microstructures of both TMP variations after heating to 633K (360°C). The grain sizes have coarsened to a size which will no longer support superplasticity.
5. Dissolution of precipitated β phase and recrystallization have taken place simultaneously and independently at the upper half of the temperature range studied.
6. The microstructure evolution study terminated at 723K (450°C) with both TMP variations exhibiting a large grain, fully recrystallized microstructure, which is not able to support superplastic deformation.
7. DSC was able to distinguish between the two TMP variations developed at NPS.

A. SUGGESTED TOPICS FOR FUTURE RESEARCH

Based on the results of this study, further investigation by differential scanning calorimetry is suggested to more fully understand the microstructural evolution in this Al-Mg-Zr alloy, and subsequently develop improved methods of microstructure control. The following topics are offered for consideration for future study using DSC:

1. Utilization of lower scanning rates, 20 K/minute and 10 K/minute, to more closely emulate the actual specimen warm-up time preceding an elevated temperature tension test.
2. Heating as rolled material at a moderate rate to temperatures at or near the superplastic deformation temperature, then monitoring the response to the isothermal condition for varying amounts of time.
3. Examination of material processed to suppress the precipitation of β which occurs during warm rolling. The effects of recrystallization can then be more directly analyzed.

LIST OF REFERENCES

1. Johnson, R.H., "Superplasticity," *Metallurgical Review*, v. 15, Review 146, pp. 115-134, 1970.

2. Underwood, E.E., "A Review of Superplasticity and Related Phenomena," *Journal of Metals*, pp. 914-919, December 1962.

3. *Metals Handbook, Desk Edition*, pp. 6.1-6.70, American Society for Metals, 1985.

4. Meyers, M.A. and Chawla, K.K., *Mechanical Metallurgy*, pp. 383-393, Prentice-Hall, 1984.

5. Smith, W.F., *Structures and Properties of Engineering Alloys*, McGraw-Hill, 1984.

6. Mondolfo, L.F., *Aluminum Alloys: Structure and Properties*, pp. 311-323,413-416,590, Butterworths, 1976.

7. Wadsworth, J., Pelton, A.R., and Lewis, R.E., "Superplastic Al-Cu-Li-Mg-Zr Alloys," *Metallurgical Transactions A*, v. 16A, pp. 2319-2332, December 1985.

8. Backofen, W.A., Turner, I.R., and Avery, D.H., *Transactions of American Society for Metals*, v. 57, p. 980, 1964.

9. Gifkins, R.C. and Langdon, T.G., "Comments on Theories of Structural Superplasticity," *Materials Science and Engineering*, v. 36, pp.27-33, 1978.

10. Sherby, O.D. and Ruano, O.A., "Synthesis and Characteristics of Superplastic Alloys," *Superplastic Forming of Structural Alloys*, Conference Proceedings of TMS-AIME and ASM 1982, pp. 241-254, The Metallurgical Society of AIME, 1982.

11. Lloyd, D.J. and Moore, D.M., "Aluminum Alloy Design for Superplasticity," *Superplastic Forming of Structural Alloys*, Conference Proceedings of TMS-AIME and ASM 1982, pp. 147-169, The Metallurgical Society of AIME, 1982.

12. Wert, J.A., "Thermomechanical Processing of Heat-Treatable Aluminum Alloys," *Microstructural Control in Aluminum Alloys: Deformation, Recovery and Recrystallization*, Symposium Proceedings of TMS-AIME 1985, pp. 67-94, The Metallurgical Society of AIME, 1986.

13. Sherby, O.D. and Wadsworth, J., "Development and Characterization of Fine-Grain Superplastic Materials," *Deformation, Processing, and Structure*, Papers presented at the 1982 ASM Materials Science Seminar, pp. 355-388, American Society for Metals, 1984.

14. Cotterill, P. and Mould, P.R., *Recrystallization and Grain Growth in Metals*, John Wiley and Sons, 1976.

15. Hull, D., *Introduction to Dislocations*, 2d ed., pp. 192-224, Pergamon Press, 1975

16. Ahlborn, H., Hornbogen, E., and Koster, U., "Recrystallization Mechanism and Annealing Texture in Aluminium-Copper Alloys," *Journal of Material Science*, v. 4, pp. 944-950, 1969.

17. Nes, E., "Strain-Induced Continuous Recrystallization in Zr-bearing Aluminium Alloys," *Journal of Material Science*, v. 13, pp. 2052-2055, 1978.

18. Watts, B.M., Stowell, M.J., Baike, B.L., and Owen, D.G.E., "Superplasticity in Al-Cu-Zr alloys Part I: Material preparation and properties," *Metal Science*, v. 10, pp. 189-197, June 1976.

19. Watts, B.M., Stowell, M.J., Baike, B.L., and Owen, D.G.E., "Superplasticity in Al-Cu-Zr alloys Part II: Microstructural study," *Metal Science*, v. 10, pp. 198-206, June 1976.

20. Grider, W.J., *The Effect of Thermomechanical Processing Variables on Ductility of a High-Mg, Al-Mg-Zr Alloy*, M.S. Thesis, Naval Postgraduate School, Monterey, California, June 1986.

21. McNaughton, J.L. and Mortimer, C.T., "Differential Scanning Calorimetry," *IRS; Physical Chemistry Series 2*, v. 10, Butterworths, 1975, reprinted with permission by Perkin-Elmer Corporation.

22. ALCOA Technical Center, Ltr., 20 August 1984.

23. Klankowski, K.A., *Retained Ambient Temperature Properties of Superplastically Deformed* Al-10%Mg-0.1%Zr, Al-10%Mg-0.5%Mn and Al-10%Mg-0.4%Cu Alloys, M.S. Thesis, Naval Postgraduate School, Monterey, California December 1985.

24. McNelley, T.R. and Garg, A., "Development of Structure and Mechanical Properties in Al-10.2 Wt. Pct. Mg by Thermomechanical Processing," *Scripta Metallurgica* v.18, pp. 917-920,1984.

25. Lendvai, J., Honyek, G., and Kovacs, I., "Dissolution of Second Phases in Al-Zn-Mg Alloy Investigated by Calorimetric Method," *Scripta Metallurgica*, v. 13, pp. 593-594, 1979.

26. Lacom, W., Degischer, H.P., Zahra, A.M., and Zahra, C.Y., "On Calorimetric and Electron Microscopic Studies of Al-Zn-Mg Alloys," *Scripta Metallurgica*, v. 14, pp. 253-254, 1980.

27. Delasi, R. and Adler, P.N., "Calorimetric Studies of 7000 Series Alloys: I. Matrix Precipitate Characterization of 7075," *Metallurgical Transactions A*, v. 8A, pp. 1177-1183, July 1977.

28. Adler, P.N. and Delasi, R., "Calorimetric Studies of 7000 Series Alloys: II. Comparison of 7075, 7050, and RX720 Alloys," *Metallurgical Transactions A*, v. 8A, pp. 1185-1190, July 1977.

29. Papazian, J.M., "The Effect of Warm Working on Aluminum Alloy 7075-T651," *Material Science and Engineering*, v. 51, pp. 223-230, 1981.

30. Papazian, J.M., "Calorimetric Studies of Precipitation and Dissolution Kinetics in Aluminum Alloys 2219 and 7075," *Metallurgical Transactions A*, v. 13A, pp. 761-769, May 1982.

31. Osamura, K. and Ogura, T., "Metastable Phases in the Early Stage of Precipitation in Al-Mg Alloys," *Metallurgical Transactions A* v. 15A, pp. 835-842, May 1984.

32. Clarebrough, L.M., Hargreaves, M.E. and Loretto, M.H., "Changes in Internal Energy Associated with Recovery and Recrystallization," *Proceedings of the Conference on the Recovery and Recrystallization of Metals,pp. 917-920, Interscience Publishers, 1963.*

33. Howe, J.M., "Metallographic and Differential Scanning Calorimetry of Precipitation and Recrystallization in an Al-Mn Alloy," *Metallurgical Transactions A*, v. 17A, pp. 593-604, April 1986.

34. Howe, J.M., "Differential Scanning Calorimetry of Aluminum Alloys," *Aluminum Alloys - Their Physical and Mechanical Properties,* Papers presented at the International Conference, v. I, pp. 603-619, Engineering Materials Advisory Services, 1986.

35. Hartman, T.S., *Mechanical Characterization of a Superplastic Aluminum-10.2%Mg-0.1%Zr Alloy*, M.S. Thesis, Naval Postgraduate School, Monterey, California, June 1985.

36. Berthold, D.B., *Effect of Temperature and Strain Rate on Microstructure of a Deformed Superplastic Al-10%Mg-0.1%Zr Alloy*, M.S. Thesis, Naval Postgraduate School, Monterey, California, June 1985.

37. McNelley, T.R., Lee, E. W., and Garg, A., "Superplasticity in Thermomechanically Processed High-Mg, Al-Mg-X Alloys," *Aluminum Alloys - Their Physical and Mechanical Properties*, Papers presented at the International Conference, v. II, pp. 1269-1283, Engineering Materials Advisory Service, 1986.

38. Nes, E., "The Effect of a Fine Particle Dispersion on Heterogeneous Recrystallization," *Acta Metallurgica*, v. 24, pp. 391-398, 1976.

39. Alcamo, M.E., *Effect of Strain and Strain Rate on the Microstructure of a Superplastically Deformed Al-10.0%Mg-0.1%Zr Alloy*, Mechanical Engineer Thesis, Naval Postgraduate School, Monterey, California, June 1985.

INITIAL DISTRIBUTION LIST

		No. Copies
1.	Defense Technical Information Center Cameron Station Alexandria, Virginia 22304-6145	2
2.	Library, Code 0142 Naval postgraduate School Monterey, California 93943-5002	2
3.	Department Chairman, Code 69Hy Department of Mechanical Engineering Naval Postgraduate School Monterey, California 93943-5000	1
4.	Professor T.R. McNelley, Code69Mc Department of Mechanical Engineering Naval Postgraduate School Monterey, California 93943-5000	5
5.	Dr. S.J. Hales, Code69Ha Department of Mechanical Engineering Naval Postgraduate School Monterey, California 93943-5000	1
6.	Naval Air Systems Command, Code AIR 931 Attn: L. Sloter Naval Air Systems Command Headquarters Washington, DC 20361	1
7.	Dr. Jeffrey Waldman, Code 606 Naval Air Development Center Warminster, Pennsylvania 18974	1
8.	Dr. Eui-Whee Lee, Code 6063 Naval Air Development Center Warminster, Pennsylvania 18974	1
9.	LCDR J.N. Andrews, USN Supervisor of Shipbuilding, Conversion, and Repair Pascagoula, Mississippi 39567	6